Thesis for the Degree of Doctor of Engineering

Optimum Bioconversion of Flavonoids from Germinated Tartary Buckwheat (*Fagopyrum tataricum* Gaertn.) using Response Surface Methodology

by

Jiyoung Shin

Department of Food Science and Technology

The Graduate School

Pukyong National University

February 19, 2021

Optimum Bioconversion of Flavonoids from Germinated Tartary Buckwheat (*Fagopyrum tatarium* Gaertn.) using Response Surface Methodology

(반응표면분석법을 이용한
발아 타타리메밀로 부터
플라보노이드의 생물전환 최적화)

Advisor: Prof. Ji-young Yang

by
Jiyoung Shin

A thesis submitted in partial fulfillment of the requirements for the degree of

Doctor of Engineering

in Department of Food Science and Technology,

The Graduate School, Pukyong National University

February 2021
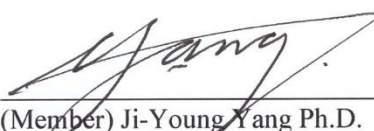
Optimum Bioconversion of Flavonoids from Germinated Tartary Buckwheat (*Fagopyrum tataricum* Gaertn.) using Response Surface Methodology

A dissertation

by

Jiyoung Shin

Approved by:

_____

(Chairman) Yang-Bong Lee Ph.D.

_____   _____

(Member) Young-Mog Kim Ph.D.   (Member) Gun-Do Kim Ph.D.

_____   _____

(Member) Sang-Gil Lee Ph.D.   (Member) Ji-Young Yang Ph.D.

February 19, 2021

CONTENTS

ii

List of Figures

List of Tables

반응표면분석법을 이용한 발아 타타리메밀로부터

플라보노이드의 생물전환 최적화

신 지 영

부경대학교 식품공학과

요 약

본 연구에서는 타타리메밀을 이용하여 발아, 추출 최적화, 생물전환을 통해 있는 플라보노이드 함량의 증진시키고자 하였다.

첫번째 연구에서는 발아 조건을 조절하여 타타리메밀싹을 제조하는 과정에서부터 플라보노이드의 함량을 높일 수 있도록 발아 조건을 달리하여 실험을 진행하였다. 기본적인 요건인 수분, 산소, 온도를 제외하고 미량성분 형성에 영향을 줄 수 있는 빛의 세기를 달리하여 실험을 진행하였다. 빛의 세기는 0 lux 에서부터 18,000 lux까지 달리하였고, 실험 결과 루틴, 쿼세틴, 미르세틴, 캠페롤의 함량은 6,000 lux에 도달할 때까지는 증가하는 경향을 나타내었다. 그리고 유사한 경향으로 총 플라보노이드 함량, 폴리페놀 함량도 증가하였고, 항산화 활성도 같이 증가하였다. 하지만, 효소 저해 활성을 통해 생리활성을

측정하는 항당뇨, 항콜레스테롤 활성은 감소하는 반대의 경향을 나타내었다. 이는 항산화 활성과는 다르게 항당뇨, 항콜레스테롤 작용하는 것이 플라보노이드 외의 다른 물질임을 알 수 있었다.

위의 조건들을 활용하여 대량 생산이 가능하도록 스마트팜 시스템을 이용한 타타리메밀싹 생산 조건을 설정하였다. 스마트팜 시스템에서는 식품으로 사용할 수 있는 제품으로의 생산을 위하여 곰팡이 등의 유해균 증식을 저해할 수 있는 조건을 찾았고, 수분을 조절할 수 있는 다양한 조건과 염소 소독 조건을 달리하여 실험을 진행하였다. 그 결과 일정량의 메밀 밀도를 가지고, 수분이 충분이 배수될 수 있는 기울기가 적합한 조건을 설정하였고, 추가적인 염소소독은 수율에 큰 영향을 미치지 않았다. 각 조건에 따른 플라보노이드 함량을 측정한 결과, 각 조건에 따라 함량에는 차이가 없었다.

재배된 타타리메밀싹에서 플라보노이드를 추출하기 위한 최적 조건을 설정하기 위하여 반응표면 분석법을 사용하였다. 독립변수로 온도, 에탄올농도, 추출 시간을 설정하였고, Box-Benhen Design을 통해 15가지의 실험 조건을 통해 값을 얻었다. 각 실험을 통해 설정된 모델은 각각의 함량의 설명하기에 충분한 값을 제시하였고, 최종적으로 루틴, 쿼세틴, 미르세틴의 함량을 최대화할 수 있는

조건으로는 51.03℃에서 69.13%의 에탄올을 이용하여 6.62시간동안 추출하는 것이었다. 이에 예측된 값은 루틴이 808.467 ㎍/mL, 쿼세틴은 193.296 ㎍/mL, 미르세틴은 37.36 ㎍/mL이었다. 이를 검증하기 위하여 10번의 반복 실험을 통해서 진행한 결과, 조금 낮은 값이 측정되었지만 충분이 예측값과 유사한 수치를 나타내었다.

추출된 플라보노이드를 이용하여 생물전환을 통해 플라보노이드의 함량을 증진시키거나, 다른 형태의 기능성을 가지는 플라보노이드를 얻기 위하여 평창의 메밀 밭에서 4가지의 균주를 분리하였다. 4가지의 균주 중에서 플라보노이드를 발효하는 균주는 *Bacillus* 속으로 추측이 되는 3P-1 이었다. 쿼세틴 200 ppm을 포함한 배지에서 3P-1을 발효하였을 때 쿼세틴의 함량은 점점 감소하고 루틴이 일정 시간 증가하였다가 감소하는 경향을 나타내었고, 미지의 물질이 발견되었고, 이 함량은 증가하는 경향을 나타내었다. 이를 분석하기 위하여 HPLC/MS를 사용하여 분자량 분석을 진행하였고, 분석결과 quercetin-3-O-glucoside를 추정되었다.

Chapter 1. General information

1.1. Buckwheat

Buckwheat belongs to the family Polygonaceae, subfamily, Polygonoideae (Zinn, 1919) in Table 1.1. It is an annual plant and dicotyledon. The origin of buckwheat is assumed River Amur in the north-east of China and around Lake Baikal in Siberia, where wild-type buckwheat was found. Historically in China, buckwheat was cultivated beginning in the Tang Dynasty and by the Song Dynasty has become widely cultivated. In Korea, buckwheat was likely cultivated beginning a long time ago because of the close geography of the country to China, with common buckwheat grown as a drought crop. Buckwheat grows well in dry soil and in areas that are cool with lower-than-average rainfall area. A crop can be raised in only 60-90 days. Buckwheat can adapt to various ecological conditions (Cai et al., 2004b).

Approximately 20 species have been discovered and classified in buckwheat worldwide (Ohnishi, 1988). The two major species are common buckwheat (Sweet buckwheat, *Fagopyrum escultum* Moench) and tartary buckwheat (bitter buckwheat, *F. tataricum* Gaertn.) (Cai et al.,

Table 1.1. Scientific classification of two buckwheat species

	Common buckwheat	Tartary buckwheat
Kingdom	Plantae	Plantae
Order	Caryophyllales	Caryophyllales
Family	Polygonaceae	Polygonaceae
Genus	*Fagopyrum*	*Fagopyrum*
Species	*F. esculentum*	*F. tataricum*

2004a) in Table 1.1. These two buckwheat species have different biological characteristics and cultivation conditions. Tartary buckwheat originated in the harsh mountainous area near Himalaya (Sytar et al., 2016; Jing et al., 2016).

The two major species also have different morphological characteristics in Fig. 1.1. Tartary buckwheat is likely more enriched in bioactive compounds, such as polyphenolic compounds, flavonoids, and vitamins. The rutin content of tartary buckwheat is approximately 100 times greater than the content of common buckwheat (Suzuki et al., 2016). The higher content of flavonoids imparts a bitter taste to tartary buckwheat (Fabjan et al., 2003). Tartary buckwheat also contains a variety of vitamins and dietary fiber. The general composition of tartary buckwheat includes 2.4% ash, 10.5% protein, 2.8% fat, 2.6% crude fiber, and 70.2% starch in the form of flour (Qin et al., 2010; Zhu, 2016). The protein content of buckwheat in general is high compared to rice and wheat. The amino acid composition of buckwheat is excellent and includes various essential amino acids, such as lysine, glutamic acid, arginine, and leucine (Bonafacci et al., 2003b; James, 1995; Javornik et al., 1984). Tartary buckwheat is a good source of vitamin B, including B_1 (thiamine), B_2, and

(A)   (B)

Fig. 1.1. Comparison of common buckwheat (A) and tartary buckwheat (B).

B$_6$, for energy metabolism (Bonafacci et al., 2003b; Zhou et al., 2015a; Zhou et al., 2015b).

1.2. Flavonoid of tartary buckwheat

Flavonoids are secondary plant phenolics that are ubiquitous in nature and in the human diet. The basic structure of flavonoids consists of 15 carbons (C$_6$-C$_3$-C$_6$). The chemical structure is diverse. Flavonoids are classified as flavonols, flavones, flavanones, catechins, anthocyanidins, isoflavones, dihydroflavonols, and chalcones. Flavonoids have potent antioxidant, free radical scavenging, antitumor, and microcirculation improving activities (Cook et al., 1996; Jing et al., 2016).

Several studies had addressed the phytochemical composition of buckwheat (Kreft et al., 2006; Jiang et al., 2007). The representative phytochemicals in tartary buckwheat are flavonoids that include rutin, quercetin, vitexin, isovitexin, and orientin. The flavonoid composition of common buckwheat is similar.

The flavonoids in buckwheat are dominated (90% of the total content) by rutin (3, 4, 5-trihydroxy-6-methyloxan-2-yl] oxymethyl] oxan-2-yl] oxychromen-4-one) in Fig. 1.2(A). Pure rutin is a pale-yellow compound

(A)   (B)

(C)   (D)
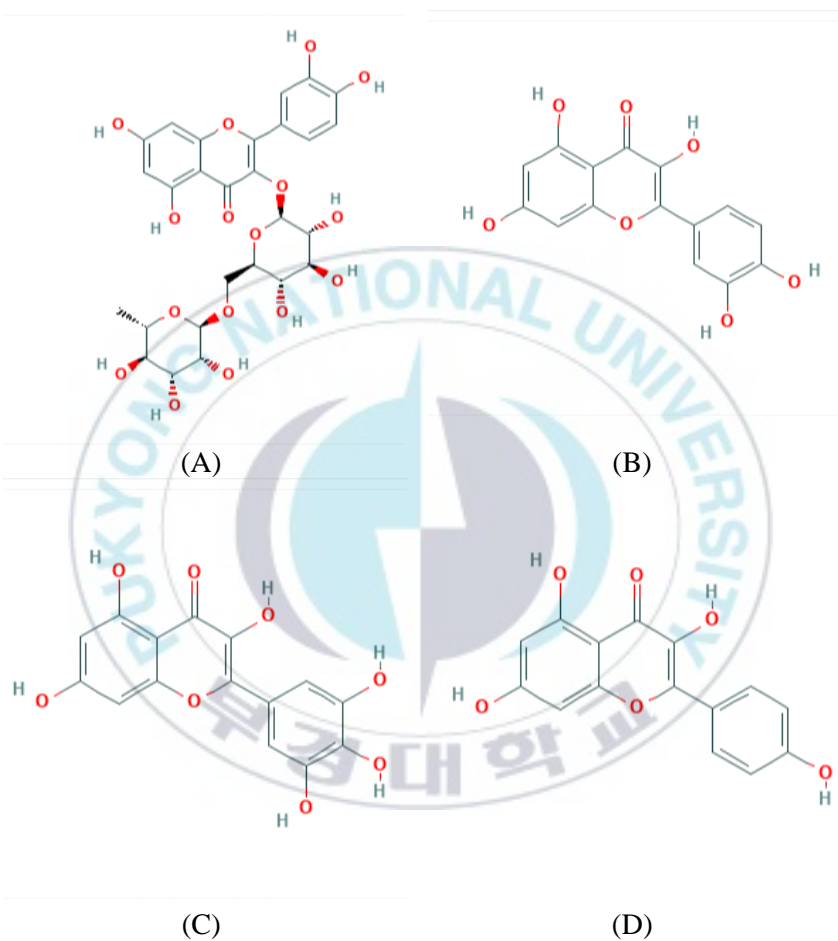
Fig.1.2. Structures of the rutin (A), quercetin (B), myricetin (C), and

kaempferol (D) major flavonoids in buckwheat.

with a molecular weight of 610.52 g/mol. It has a low aqueous solubility of 12.5 mg/100 g. Rutin accounts for 90% of the antioxidant activity in tartary buckwheat (Ladan et al., 2017). During food processing, rutin is degraded to quercetin and L-rhamnose by rutin degrading enzyme. The degradation increases the bitter taste (Tranchimand et al., 2010). The various physiological activities of rutin include antioxidant, antimicrobial, anti-inflammatory, anticancer, antidiabetic, antihypertensive, antiallergic, and antithrombogenic activities. Rutin is used as a nutritional supplement because of its remediation activities for oxidative stress, inflammation, and hyperglycemia. However, despite its many bioactivities, the use of rutin has been hampered by its low water solubility. Diverse research has sought to overcome this solubility problem. Attempts to improve solubility have included nanoparticle systems, enzymatic oligomerization acylation, and chemical reactions to generate hydroxyethyl, carboxylate, and sulfonate derivatives (Gullon et al., 2017).

Quercetin (2-(3,4-dihydroxyphenyl)-3,5,7-trihydroxychromen- 4-one) in Fig. 1.2(B) is one of a group of over 4000 natural phenolic compounds that are present in many vegetable, fruits, grains, and seeds. Typically, the concentration of quercetin is high in the edible portions of

some foods, such as apples, onions, kale, French beans, broccoli, lettuce, and tomatoes (Formica et al., 1995; Hertog et al., 1992). Many studies have examined quercetin because it is a predominant flavonoid in foods (Cook et al., 1996). Quercetin has antioxidant, anticarcinogenic, anti-inflammatory, anti-aggregatory, and vasodilatory effects. The antioxidant aspects of quercetin include metal chelation, scavenging of radicals, enzyme inhibition, and induction of the expression of protective enzymes (Erlund, 2004). After metabolic conversion of quercetin, the biological activities are decreased, but the bioactive compound aglycone is generated. Quercetin aglycone modulates several signal transduction pathways during apoptosis in inflammation and carcinogenesis (Murakami et al., 2008; Nguyen et al., 2004).

Myricetin (3, 5, 7-trihydroxy-2-(3, 4, 5-trihydroxyphenyl) chrom en-4-one) in Fig. 1.2(C) is a flavonoid with hydroxyl substitutions at the 3, 5, 7, 3', 4', and 5' positions (Ong et al., 1997). Myricetin naturally exists as a bioflavonoid that is widespread naturally among plants, including vegetables, berries, tea, and medicinal herbs (Hertog et al., 1993a). Myricetin is a very effective antioxidant in the treatment of obesity and obesity-related metabolic disorders (Xia et al., 2016). It is commonly

consumed as it is present in vegetables, fruits, tea, and wine (Hertog et al., 1993b). The functional properties of myricetin include potent antioxidant activity (Robak et al., 1998a; Robak et al., 1998b), anticarcinogenic activity (Hertog et al., 1993b), and prevention of platelet aggregation (Tzeng et al., 1991). The antioxidant activity is paramount. Myricetin is effective in scavenging radicals generated by both enzymatic and nonenzymatic systems (Ong et al., 1997).

Kaempferol (3, 5, 7-trihydroxy-2-(4-hydroxyphenyl) chromen -4-one) in Fig. 1.2(D) is a flavonoid that is a yellow compound in its pure form. It has a low molecular weight of 286.2 g/mol. Kaempferol is a constituent of many plants and plant-derived foods, including broccoli, apples, strawberries, kale, tea, spinach, and beans (Chen et al., 2013; Holland et al., 2020; Sornerset et al., 2008). Kaempferol has antioxidant, anti-inflammatory, anti-cancer, and antimicrobial activities. One study describes a role of kaempferol in reducing cardiovascular diseases (Calderon-Montano et al., 2011). The antioxidant activity of kaempferol includes superoxide and hydroxyl radical scavenging (Wang et al., 2006). The antioxidant activity relies on a double bond with the conjugation with an oxo group and hydroxyl group. Kaempferol inhibits nuclear factor

kappa B (NF-κB), whose activation increases cytokine, chemokines, and enzymes involved in inflammatory responses. A role for kaempferol as an anti-cancer agent that involves protection of DNA from damage mediated by carcinogens has been described (Cemeli et al., 2004). Tartary buckwheat contains other flavonoids. This study focused on rutin, quercetin, myricetin, and kaempferol.

1.3. Germination

Germination is a complex process during which the seed grows into the young plant. The seed has to physically recover from maturation to break through the seed coat and prepare for subsequent growth (Nonogaki et al., 2010).

Germination is an effective method to enhance the nutritional value of cereal. The germination process is complex and produces significant differences in biochemical, nutritional, and organoleptic characteristics by activating several enzymes. When seeds are germinated and grown as sprouts, they have a much higher nutritional value than the original seeds (Zhang et al., 2015).

During the germination, the general composition of grain changes,

including carbohydrate, protein, and lipid. Changes also involve bioactive compounds, such as pigment compounds (including flavonoids, anthocyanin, and others) and enzymes. Grains and seeds need enzymes for functions that include photosynthesis in order to manufacture nutrients for germination and growth.

Carbohydrate is decreased, and crude protein, ash, and lipid are increased in germinated buckwheat. During germination period, the rutin and vitamin C contents increase continuously (Lee et al., 2008). Thus, germination is an excellent condition to improve bioactive compounds.

1.4. Bioconversion

Bioconversion is the chemical conversion of organic material to useful sources of energy and other aspects. The process involves physiologic functions of the microbe and its' constituent enzymes. Microbial transformation is a type of bioconversion. It is a useful technology to produce new compounds. In microbial bioconversion, an organic compound is converted to a structurally related compound through one or several enzymatic reactions (Perkins et al., 2015). Enzyme-catalyzed microbial bioconversion has been used for centuries to

manufacture foods, beverages, food supplements, and medicines. Commercially, bio-products that include vitamin derivatives and flavonoids are manufactured by bioconversion. In addition, bioconversion is an environmentally friendly way to convert waste into energy.

Food bioconversion is the transformation of food material by biological processes. Bioconversion technologies include immobilized enzymes, fermentation, and hydrolysis. Bioconversion is used to manufacture enzymes, organic acids, amino acids, polysaccharides, alcohols, aroma compounds, and pigments in food industries (Norton et al., 1994).

1.5. Objectives of this study

The pharmacological mechanisms of bioactive ingredients from medicinal plants have been established. This knowledge has enabled research on functional foods and supplement development using natural resources. This study aimed to enhance flavonoid content and functionality by controlling the conditions of germination, extraction, and bioconversion of flavonoids using tartary buckwheat sprouts. Specifically, the followings were performed:

- Enhancing flavonoid content during germination by controlling the light strength and establishment of germination condition using a smart farm system for the commercial manufacture of tartary buckwheat sprouts (Chapter 2)

- Optimization of the extraction of the rutin, quercetin, and myricetin flavonoids using response surface methodology (RSM) (Chapter 3)

- Enhancing flavonoid composition throughout bioconversion using isolated bacteria to improve functionality (Chapter 4)

1.6. References

Bonafaccia G, Marocchini M, Kreft I. 2003. Composition and technological properties of the flour and bran from common and tartary buckwheat. Food Chemistry, 80, 9-15.

Cai Y, Corke H, Li W. 2004a. Buckwheat. In:'Encyclopedia of Grain Science. Oxford. Elsevier. pp120-128.

Cai Y, Luo Q, Sun M, Corke H. 2004b. Antioxidant activity and phenolic compounds of 112 traditional Chinese medicinal plants associated with anticancer. Life Sciences, 74, 2157-2184.

Cemeli E, Schmid TE, Anderson D. 2004. Modulation by flavonoids of DNA damage induced by estrogen-like compounds. Environmental and Molecular Mutagenesis, 44, 420-426.

Chen AY, Chen YC. 2013. A review of the dietary flavonoid, kaempferol on human health and cancer chemoprevention. Food Chemistry, 138, 2099-2107.

Cook NC, Samman S. 1996. Flavonoids—chemistry, metabolism, cardioprotective effects, and dietary sources. The Journal of Nutritional Biochemistry, 7, 66-76.

Erlund I. 2004. Review of the flavonoids quercetin, hesperetin, and naringenin. dietary sources, bioactivities, bioavailability, and epidemiology. Nutrition Research, 24, 851-874

Fabjan N, Rode J, Košir IJ, Wang Z, Zhang Z, Kreft I. 2003. Tartary buckwheat (*Fagopyrum tataricum* Gaertn.) as a source of dietary rutin and quercitrin. Journal of Agricultural and Food Chemistry, 51, 6452-6455.

Formica JV, Regelson W. 1995. Review of the biology of quercetin and related bioflavonoids. Food and Chemical Toxicology, 33, 1061-1080.

Gullon B, Lu-Chau TA, Moreira MT, Lema JM, Eibes G. 2017. Rutin: A review on extraction, identification and purification methods, biological activities and approaches to enhance its bioavailability. Trends in Food Science and Technology, 67, 220-235.

Hertog MG, Feskens EJ, Kromhout D, Hollman PCH, Katan MB. 1993a. Dietary antioxidant flavonoids and risk of coronary heart disease: the Zutphen Elderly Study. The Lancet, 342, 1007-1011.

Hertog MG, Hollman PC, Katan MB, Kromhout D. 1993b. Intake of potentially anticarcinogenic flavonoids and their determinants in adults in The Netherlands. Nutrition and Cancer, 20, 21-29.

Hertog MG., Hollman PC, Katan MB. 1992. Content of potentially anticarcinogenic flavonoids of 28 vegetables and 9 fruits commonly consumed in the Netherlands. Journal of Agricultural and Food Chemistry, 40, 2379-2383.

Holland TM, Agarwal P, Wang Y, Leurgans SE, Bennett DA, Booth SL, Morris MC. 2020. Dietary flavonols and risk of Alzheimer Dementia. Neurology, 94, e1749-e1756.

James U. 1995. Buckwheat: The wonderful nutritional values of buckwheat. In Pro. 6th Internationl Symposium Buckwheat at

Ina. pp1027-1029.

Javornik B, Kreft I. 1984. Characterization of buckwheat proteins. Fagopyrum, 4, 30-38.

Jiang P, Burczynski F, Campbell C, Pierce G, Austria JA, Briggs CJ. 2007. Rutin and flavonoid contents in three buckwheat species *Fagopyrum esculentum*, *F. tataricum*, and *F. homotropicum* and their protective effects against lipid peroxidation. Food Research International, 40, 356-364.

Jing R, Li HQ, Hu CL, Jiang YP, Qin LP, Zheng CJ. 2016. Phytochemical and pharmacological profiles of three *Fagopyrum* buckwheats. International Journal of Molecular Sciences, 17, 589.

Kreft I, Fabjan N, Yasumoto K. 2006. Rutin content in buckwheat (*Fagopyrum esculentum* Moench) food materials and products. Food Chemistry, 98, 508-512.

Lee EH, Kim CJ. 2008. Nutritional changes of buckwheat during germination. Journal of the Korean Society of Food Culture, 23, 121-129.

Nguyen TTT, Tran E, Nguyen TH, Do PT, Huynh TH, Huynh H. 2004. The role of activated MEK-ERK pathway in quercetin-induced

growth inhibition and apoptosis in A549 lung cancer cells. Carcinogenesis, 25, 647-659.

Nonogaki H, Bassel GW, Bewley JD. 2010. Germination—still a mystery. Plant Science, 179, 574-581.

Norton S, Vuillemard JC. 1994. Food bioconversions and metabolite production using immobilized cell technology. Critical Reviews in Biotechnology, 14, 193-224.

M Calderon-Montano J, Burgos-Moron E, Perez-Guerrero C, Lopez-Lazaro M. 2011. A review on the dietary flavonoid kaempferol. Mini Reviews in Medicinal Chemistry, 11, 298-344.

Murakami A, Ashida H, Terao J. 2008. Multitargeted cancer prevention by quercetin. Cancer Letters, 269, 315-325.

Ohnishi O. 1988. Population genetics of cultivated common buckwheat, *Fagopyrum esculentum* Moench. The Japanese Journal of Genetics, 63, 507-522.

Ong KC, Khoo HE. 1997. Biological effects of myricetin. General Pharmacology: The Vascular System, 29, 121-126.

Qin P, Wang Q, Shan F, Hou Z, Ren G. 2010. Nutritional composition and flavonoids content of flour from different buckwheat

cultivars. International Journal of Food Science and Technology, 45, 951-958.

Robak J, Korbut R, Shridi F, Swies J, Rzadkowska-Bodalska H. 1988a. On the mechanism of antiaggregatory effect of myricetin. Polish Journal of Pharmacology and Pharmacy, 40, 337-340.

Robak J, Shridi F, Wolbis M, Krolikowska M. 1988b. Screening of the influence of flavonoids on lipoxygenase and cyclooxygenase activity, as well as on nonenzymic lipid oxidation. Polish Journal of Pharmacology and Pharmacy, 40, 451-458.

Somerset SM, Johannot L. 2008. Dietary flavonoid sources in Australian adults. Nutrition and Cancer, 60, 442-449.

Suzuki T, Morishita T. 2016. Bitterness generation, rutin hydrolysis, and development of trace rutinosidase variety in tartary buckwheat. Molecular Breeding and Nutritional Aspects of Buckwheat. Academic Press. pp345-353.

Perkins C, Siddiqui S, Puri M, Demain AL. 2016. Biotechnological applications of microbial bioconversions. Critical Reviews in Biotechnology, 36, 1050-1065.

Tranchimand S, Brouant P, Iacazio G. 2010. The rutin catabolic pathway

with special emphasis on quercetinase. Biodegradation, 21, 833-859.

Wang L, Tu YC, Lian TW, Hung JT, Yen JH, Wu MJ. 2006. Distinctive antioxidant and antiinflammatory effects of flavonols. Journal of Agricultural and Food Chemistry, 54, 9798-9804.

Xia SF, Le GW, Wang P, Qiu YY, Jiang YY, Tang X. 2016. Regressive effect of myricetin on hepatic steatosis in mice fed a high-fat diet. Nutrients, 8, 799.

Zhang G, Xu Z, Gao Y, Huang X, Zou Y, Yang T. 2015. Effects of germination on the nutritional properties, phenolic profiles, and antioxidant activities of buckwheat. Journal of Food Science, 80, 1111-1119.

Zhu F. 2016. Chemical composition and health effects of Tartary buckwheat. Food Chemistry, 203, 231-245.

Zhou X, Hao T, Zhou Y, Tang W, Xiao Y, Meng X, Fang X. 2015a. Relationships between antioxidant compounds and antioxidant activities of tartary buckwheat during germination. Journal of Food Science and Technology, 52, 2458-2463.

Zhou Y, Wang H, Cui L, Zhou X. Tang W, Song X. 2015b. Evolution of nutrient ingredients in tartary buckwheat seeds during germination.

Food Chemistry, 186, 244-248.

Zinn, J. 1919. On variation in tartary buckwheat, *Fagopyrum tataricum* (L.) Gaertn. Genetics, 4, 534.

Chapter 2. Germination of tartary buckwheat
at various light strengths to enhance flavonoid content
and scale-up of the process

Abstract

To evaluate the relationship between light strength and bioactive compounds of tartary buckwheat sprouts, sprouts were germinated and grown using different light strengths. The contents of rutin and other flavonoids increased until 6,000 lux. Total flavonoid and polyphenol contents were highest at 10,000 lux. Antioxidant activity had a similar tendency as flavonoid contents concerning light intensity. Anti-glycemic and anti-cholesterol activities displayed opposite tendencies. While 6,000 lux was the best condition for flavonoid contents, this light intensity is not feasible at industrial scale. For the scale-up of sprout production, the smart farm system was used and optimal conditions were established. The optimal conditions considering yield and productivity were 600 g tartary buckwheat per plate, 5° slope, and no choline sterilization. Flavonoid contents were not affected by these conditions.

21

2.1. Introduction

Many nutritional and bioactive compounds in seeds and grains are altered during germination. The starch composition tends to increase in barley, buckwheat, oats, sorghum, and brown rice, but does not in wheat and rye. The protein contents of all grains are increased after germination. Bioactive compounds, such as gallic acid, epigallocatechin, catechin, epicatechin, epigallocatechin gallate, ρ-coumaric acid, ferulic acid, and luteolin, increase during the germination of barley, rye, sorghum, and wheat (Donor et al., 2012; Fabjan et al., 2003). After germination of brown rice, the crude protein content, sugar, reducing sugar, and free amino acid significantly increase (Moongngarm et al., 2010). In a study comparing the chemical composition of safflower seeds before and after germination, α-tocopherol increased from 744.7 mg% (dry base) to 809.0 mg%, and the contents of total and essential amino acids tended to increase. Also, saturated fatty acid (palmitic acid, stearic acid, and oleic acid) content decreased, while unsaturated fatty acid (linoleic acid and arachidic acid) was increased slightly (Kim et al., 2008).

A previous study reported that germination enhanced nutritional value, including bioactive compounds. The content of bioactive rutin was

increased during the germination of both common and tartary buckwheat germination. Many studies have sought to clarify the relationship between light and bioactive compounds. However, no study has investigated the relationship between light strength and bioactive compounds before and after germination.

Microgreens refer to salad crop shoots that are harvested for consumption within 20 days. Microgreens are also called sprout and baby salads (Murphy et al., 2010). Manufacturing microgreens requires controlled germination conditions. Different germination conditions that include temperature and water contents are needed depending on the grain and seed characteristics. The germination conditions also need to protect sprouts from contamination by fungi and bacteria, since the sprouts are destined for consumption, usually raw.

For the industrial-scale manufacture of sprouts, a smart farm system was used. A smart farm system can control the condition of the farm automatically using Information and Communication Technology and the Internet of Things. When setting the germination condition for each grain or seed, the water, light, and drainage conditions can be controlled during the cultivation period. This system is more convenient than the

conventional method. The strengths of this system (Bonafaccia et al., 2003) include the automatic control of the conditions (Gulpinar et al., 2012), smaller space (Yoon et al., 2012), less labor (Zhang et al., 2012), and the ability to cultivate crops in a sterilized condition that is not affected by the weather.

This study aimed to enhance rutin and other flavonoid content by controlling germination and growth light conditions during the manufacture of buckwheat sprouts. Bioactive properties were determined in extracts of tartary buckwheat sprouts grown under different light strengths. The study also sought to optimize the growth conditions with the goal of the scaled-up manufacturing tartary buckwheat sprouts using a smart farm system.

2.2. Materials and methods

2.2.1. Materials

Common buckwheat and tartary buckwheat were grown on Jeju Island, South Korea. The solvents for HPLC, including acetonitrile (ACN), methanol, water, and acetic acid, were purchased from J.T. Baker (Phillipsburg, NJ, USA). Folin–Ciocalteu reagent was purchased from

Sigma-Aldrich Chemical Co. (St. Louis, MO, USA). Rutin, kaempferol, quercetin, myricetin and gallic acid were purchased from Sigma-Aldrich Chemical Co. as standard analytical grade compounds.

2.2.2. Germination of tartary buckwheat

Tartary buckwheat was grown under high light intensity to investigate the influence of germination and growth light conditions on flavonoid contents. A model JSPC-420C biological growth chamber (JS Research Inc., Gongju, Republic of Korea) was used to control light, temperature, and relative humidity.

Tartary buckwheat was soaked for 24 h at 20°C and put in a germination box. Germination occurred during the first 24 h at 20°C. Tartary buckwheat was grown in the growth chamber at 20°C and 99% relative humidity under different light intensities of 0, 500, 4,000, 8,000, 12,000 16,000, 18,000, and 22,000 lux. The sprouts of tartary buckwheat were dried using a hot-air dryer at 40°C for 24 h. The dried sprouts were stored at -80°C until required.

2.2.3. Extraction of tartary buckwheat sprout

The dried tartary buckwheat sprouts were extracted using ethanol. One gram of the dried sprouts was immersed in 20 mL ethanol in a 50 mL conical tube. Extraction was performed in a constant temperature water tank with shaking at 130 rpm at 30°C for 3 h. The extracts were filtered through No. 3 quantitative filter paper (Adventec, Tokyo, Japan). The filtrates were stored at 4°C until required.

2.2.4. Total flavonoid content

The total flavonoid content was measured as described by previous study with some modification (Moreno et al., 2000). Briefly, 20 μL of sample, 4 μL of 10% aluminum nitrate, 4 μL of 1 M potassium acetate, and 172 μL of ethanol were mixed in each well of a 96-well plate. The mixture was left at room temperature for 40 min in the dark. The absorbance was measured at 415 nm using a microplate reader. The standard curve was prepared with quercetin (Sigma-Aldrich) at concentrations of 0 to 100 μg/mL.

2.2.5. Total polyphenol content

The total polyphenol content of DTBS samples was measured by the

Folin–Denis method using Folin–Ciocalteu reagent (Sigma-Aldrich). Briefly, 50 μL of sample extract or standard was mixed with 20 μL of 50% Folin–Ciocalteu phenol reagent in each well of a 96-well plate and left at room temperature for 3 min. Then, 30 μL of 10% Na_2CO_3 solution was added and the mixture was left at room temperature for 30 min. One hundred microliters of distilled water was added to terminate the reaction. Absorbance was measured at 750 nm using a microplate reader (EPOCH2; BioTek Instruments, Inc., Winooski, VT, USA). The standard curve was prepared with gallic acid (Sigma-Aldrich) at concentrations of 0 to 100 μg/mL.

2.2.6. Flavonoid content analysis using HPLC

Flavonoid content was analyzed by HPLC using a model U-3000 device (Thermo Fisher Scientific Inc., Waltham, MA, USA). Before analysis, all samples were filtered through a 0.45 μm cellulose acetate syringe filter (Adventec, Tokyo, Japan).

The analysis column was an Acclaim C18 column (250×4.6 mm, 5 μm, Thermo Fisher Scientific Inc.), and mobile phases were 0.03 M phosphoric acid (A) and methanol (B) eluted using the following gradient:

0 min, 60% A; 10 min 0% A; 15 min 0% A; 20 min 60% A; 25 min 60% A. The flow rate was 1.0 mL/min, and the detection wavelength was 360 nm. The detailed conditions are provided in Table 2.1. The calibration curve was used to simultaneously quantify rutin, quercetin, kaempferol, and myricetin under the described analytical conditions.

2.2.7.   Antioxidant activity

2.2.7.1. DPPH radical scavenging activity.

1, 1-Diphenyl-2-picrylhydrazyl (DPPH) radical scavenging activity was measured as described by Sharma and Bhat (2009) with some modifications. DPPH (0.078 g) was dissolved in 1 L methanol. Samples (100 μL) of and 100 μL of the DPPH solution were added to each well of a 96-well plate and left in a dark room at 35°C for 30 min. The absorbance was measured at 517 nm using the aforementioned EPOCH2 microplate reader. The same amount of methanol as the sample solution was used as the negative control. Ascorbic acid (100 ppm) in methanol was used as the positive control. The samples were diluted 1/100. DPPH radical scavenging activity (%) was calculated as:

Table 2.1. HPLC conditions for analysis of flavonoids

		Condition	
	Model	Acclaim™ 120	
Column	Size	4.6×250 mm	
	Particle size	5 μm	
	Flow rate	1 ml/min	
	Retention time	0.03 M Phosphoric acid	Methanol
	0	60	40
	10	0	100
Analysis condition	15	0	100
	20	60	40
	25	60	40
	UV detector	350 nm	
	Injection quantity	20 μL	

Radical scavenging activity (%)

$$= \frac{\text{Absorbance}_{(\text{blank})} - \text{Absorbance}_{(\text{test})}}{\text{Absorbance}_{(\text{blank})}} \times 100$$

2.2.7.2. ABTS radical scavenging activity

2, 2′-Azinobis-(3-ethylbenzothiazoline-6-sulfonic acid (ABTS) radical scavenging activity was measured using an antioxidant assay kit (Sigma-Aldrich). Ten microliters of sample and 20 μL of myoglobin working solution were added to each well of a 96-well plate, followed by 150 μL of ABTS substrate working solution. The plate was left at room temperature for 5 min. One hundred microliters of stop solution was added to each well terminate the reaction, and the absorbance was measured at 405 nm using the aforementioned EPOCH2 microplate reader. The samples were diluted 1/100. The standard curve was prepared using a working solution of Trolox with assay buffer, adjusting the concentration from 0 to 0.42 mM.

2.2.7.3. FRAP assay

The Ferric Antioxidant Power (FRAP) assay was performed as

described by Benzie and Strain (1996), with previously described modifications (Benzie et al., 1996; Thaipong et al., 2006). The stock solutions included 300 mM acetate buffer (3.1 g $C_2H_3NaO_2 \cdot 3H_2O$ and 16 mL $C_2H_4O_2$; pH 3.6), 10 mM 2, 4, 6-tripyridyl-s-triazine (TPTZ) solution in 40 mM HCl, and 20 mM $FeCl_3 \cdot 6H_2O$ solution. The working solution comprised 25 mL acetate buffer, 2.5 mL TPTZ solution, and 2.5 mL $FeCl_3 \cdot 6H_2O$ solution. The solution was warmed at 37°C before use. Tartary buckwheat sprout extract (150 μL) was reacted with 2850 μL of the FRAP solution for 30 min in the dark. The absorbance of the colored product (ferrous tripyridyltriazine complex) was measured at 593 nm using the aforementioned EPOCH2 microplate reader. The standard curve was linear between 0 and 250 μM $FeSO_4$. Results are expressed in μmol $FeSO_4$/mL. Additional dilution was done if the FRAP value measured exceeded the linear range of the standard curve.

2.2.8. Anti-glycemic activity

2.2.8.1. α-Glucosidase inhibition activity

The α-glucosidase inhibition activity of extracts of tartary buckwheat sprout was measured as previously described with some modifications

31

(Dong et al., 2012; Qin et al., 2017; Sheliya et al., 2015). Briefly, 50 μL of each sample extract and 50 μL of 100 mM phosphate buffer (pH 6.8) containing α-glucosidase solution (0.2 U/mL) were incubated in 96-well plates. After pre-incubation at 37°C for 10 min, 50 μL of 5 mM p-nitrophenyl-α-d-glucopyranoside (PNPG) substrate solution in 0.1 M phosphate buffer (pH 6.8) was added to each well and incubated at 37°C for 20 min. After incubation, the reaction was terminated by adding 160 μL of 0.2 M NaCO₃ to each well. The absorbance of the reactant was measured at 405 nm using the aforementioned EPOCH2 microplate reader. The control was 50 μL of buffer solution instead of the sample. The α-glucosidase inhibitory activity was expressed as inhibition % and was calculated as:

α-Glucosidase inhibition activity (%)

$$= \frac{\text{Absorbance}_{(\text{control})} - \text{Absorbance}_{(\text{sample})}}{\text{Absorbance}_{(control)}} \times 100$$

The concentration of inhibitors required to inhibit 50% of the α-glucosidase activity under the assay conditions was defined as the IC_{50} value.

2.2.8.2. α-Amylase inhibition activity

α-Amylase inhibitory activity was measured according to methods described by a previous study with slight modifications. Forty microliters of the sample was mixed with 200 μL of α-amylase solution (1.0 U/mL in the pH 6.9 buffer) and pre-incubation at 25°C for 10 min. Then, 400 μL of a 0.25% starch solution was added to each tube. The reaction occurred at 37°C for 5 min. The reaction was terminated by adding 1.0 mL of a solution containing 1% 3, 5-dinitrosalicylic acid (DNS) and 12% sodium potassium tartrate in 0.4 M NaOH. The test tubes were placed in a boiling water bath for 5 min and cooled to room temperature. The reaction mixture was then diluted using distilled water in wells of a 96-well plate, and absorbance was measured at 540 nm using the aforementioned EPOCH2 microplate reader. The control had 200 μL of buffer solution in place of the α-amylase solution. The % inhibition was calculated as:

α-Amylase inhibition activity (%)

$$= \frac{\text{Absorbance}_{(\text{control})} - \text{Absorbance}_{(\text{sample})}}{\text{Absorbance}_{(control)}} \times 100$$

2.2.9. Assay of human HMG-CoA reductase activity

Human HMG-CoA reductase (HMGR) activity and inhibition assays were carried out using the HMGR Assay Kit from Sigma-Aldrich (SigmaCS-1090) according to the recommended instructions by the manufacturer and as previously described (Mendieta et al., 2014; Soares et al., 2015). The kit was designed to detect HMGR activity. Pravastatin was used as a positive control. Briefly, 4 μL of NADPH (final concentration 400 mM) and 12 μL of HMG-CoA substrate (final concentration 0.3 mg/mL) were added to wells of a 96-well plate. The final volume in each well was 0.2 mL by adding 1× phosphate assay buffer (pH 7.4). The reaction was started by the addition of 2 μL of the HMG-CoA reductase (concentration of the enzyme stock solution was 0.50–0.70 mg protein/mL) followed by incubation at 37°C in the presence or absence of 1 μL pravastatin (control) or an equal volume of the samples (Mendieta et al., 2014; Soars et al., 2015). NADPH was measured every 20 s for 10 min by determining the absorbance at 340 nm using the aforementioned EPOCH2 microplate reader. The inhibitory activity results were expressed as 1.0 μmol NADPH to $NADP^+$ per min at 37°C in the presence or the absence of pravastatin or samples.

2.2.10. Scale-up of germination using the smart farm system

Tartary buckwheat was cultivated in 2015 on Jeju Island and was stored at room temperature. The smart farm system was used in the smart farm factory (Boram E&G, Hoeng-seong, Kangwonwdo, Republic of Korea). The smart farm system is shown in Fig. 2.1. The size of the plate was 30×90 cm. The light strength was 200 lux.

One kilogram of tartary buckwheat was soaked for 24 h and drained. The buckwheat was put on the smart farm germination plate and germinated.

The initial attempt was for 12 days. During this germination period, fungi contamination of the tartary buckwheat sprouts occurred. To remedy this, the density of tartary buckwheat in the plate was changed to reduce non-germinated tartary buckwheat and the plate angle was changed to lower the water holding capacity in the roots of tartary buckwheat sprouts in the plate. Tartary buckwheat amounts of 0.4, 0.6, and 0.8 kg were used. In addition, the plate angle (5 and 7°) was adjusted to regulate the drainage speed to reducing water holding capacity. Chlorinated water was applied as a spray once each day to prevent contamination. The various yield conditions are summarized in Table 2.2. The yield (%) was calculated as:
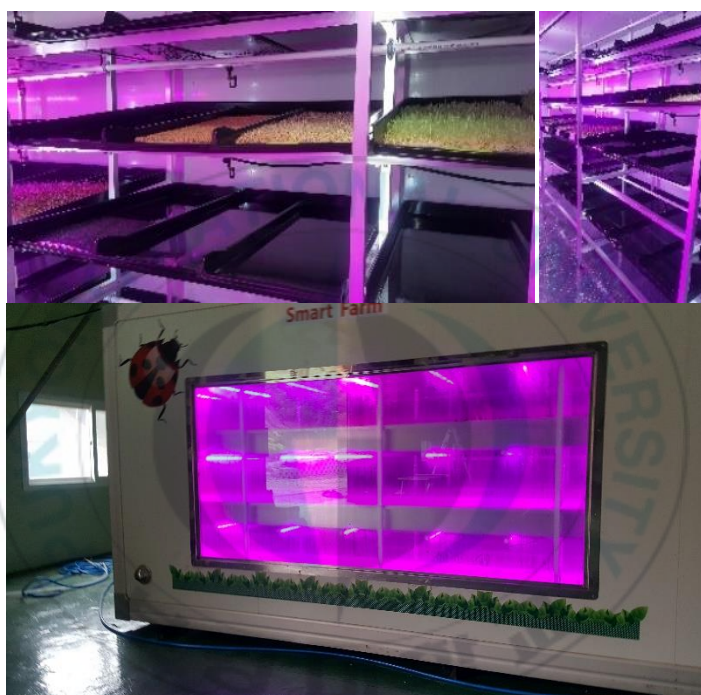
Fig. 2.1. Smart farm system for germination of tartary buckwheat.

Table 2.2. Germination conditions using the smart farm system

		Slope (°)	Chlorine sterilization
1	400	5	×
2	400	7	×
3	600	5	×
4	600	7	×
5	600	5	○
6	600	7	○
7	800	5	×
8	800	**7**	×

Yield (%)

$$= \frac{\text{Weight of sprouts}}{\text{Weight of inoculated tartary buckwheat}} \times 100$$

2.2.11. Statical analysis

All determinations were performed in triplicate. Statistical analyses were conducted by one-way analysis of variance (ANOVA) using Minitab M16 software. Differences with a p-value <0.05 were considered significant.

2.3. Results and discussions

2.3.1. Morphological characteristics of tartary buckwheat sprouts germinated using different light strength

The morphological characteristics of tartary buckwheat sprouts are shown in Fig. 2.2. When observed with the naked eye, the leaves of sprouts became greener with increasing light strength, and the stems of the sprouts became redder. Tsurunaga et al. (2013) described differences in the color of leaves and stems of buckwheat sprouts grown under different wavelengths of light, including white, red, green, blue, and ultraviolet (UV)
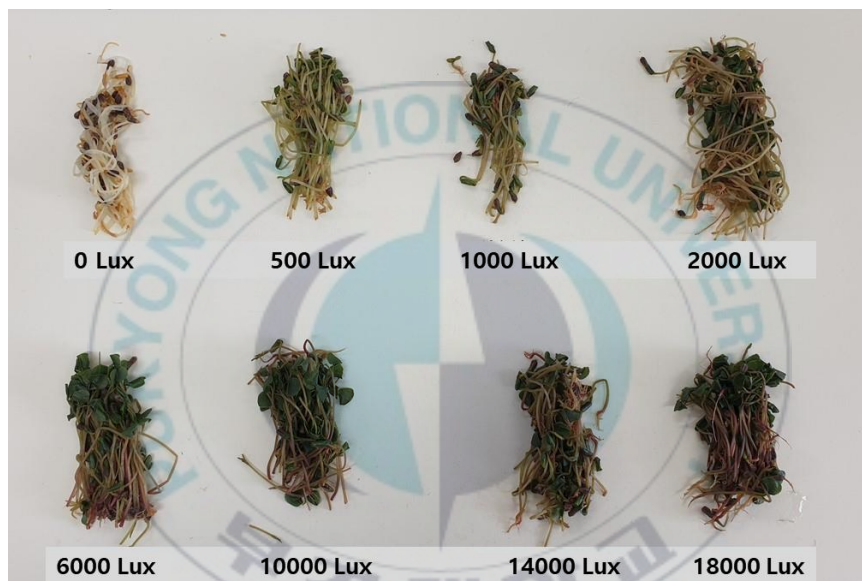
Fig. 2.2 Morphological characteristics of sprouts germinated under the different light strengths.

light. The authors also noted that stems irradiated with UV-B were the reddest. The germination using common buckwheat in the fluorescent, red, blue, and dark light conditions was similar to this study. Sprouts grown in the dark were reported to be the longest (Nam et al. 2018a). Waterland and Moon (2017) described that three different cultivars of kale had different colors according to their genetic differences and growth stage. Mineral content and water content also differed. Plant color, especially that of sprouts (microgreen), could indicate different nutritional compositions. However, it was not observed increased length of tartary buckwheat sprouts under high intensity light. As the light intensity increased, the length of tartary buckwheat sprouts became shorter. Previous research to investigate the relationship between light-emitting diode (LED) radiation and pea seedlings discovered that stem length and weight were affected by light intensity. Seeds grown in the dark were longer than seedlings grown in the light (Wu et al., 2007). These observations had a similar tendency to the present study, in that the sprouts in the dark were the longest. However, cultivating sprouts in the dark was not recommended only for length growth. It was necessary to decide the germination condition according to the purpose of the sprouts.

2.3.2. Flavonoid content of tartary buckwheat sprouts grown at the different light strengths

The standard peaks of each flavonoid analyzed by HPLC are shown in Fig. 2.3. Rutin, myricetin, quercetin, and kaempferol were evident at 6.607 min, 7.467 min, 8.680 min, and 9.720 min, respectively. The analysis condition completely resolved each flavonoid.

Fig. 2.4 displays the findings of the rutin content of tartary buckwheat sprouts grown under the different light strengths. The rutin content tended to increase as the light intensity increased until it reached 6,000 lux. At light strengths over 8,000 lux, rutin content decreased slightly. The rutin content of tartary buckwheat sprouts grown in 0 lux (in the dark) and 6,000 lux was 883.87 mg/L and 1,184.33 mg/L, respectively. Tartary buckwheat sprouts grown at 14,000 and 18,000 lux showed similar rutin content to sprouts grown at 0 lux. The findings indicated that the highest rutin content could be attained by growth of tartary buckwheat sprouts at 6,000 lux. In a previous study of germinating common buckwheat, the rutin content of sprouts grown in blue light was 2.5-fold higher than in sprouts grown in the dark. Moreover, sprouts grown in red and fluorescent light had 2-times higher rutin content than those grown in the dark (Nam
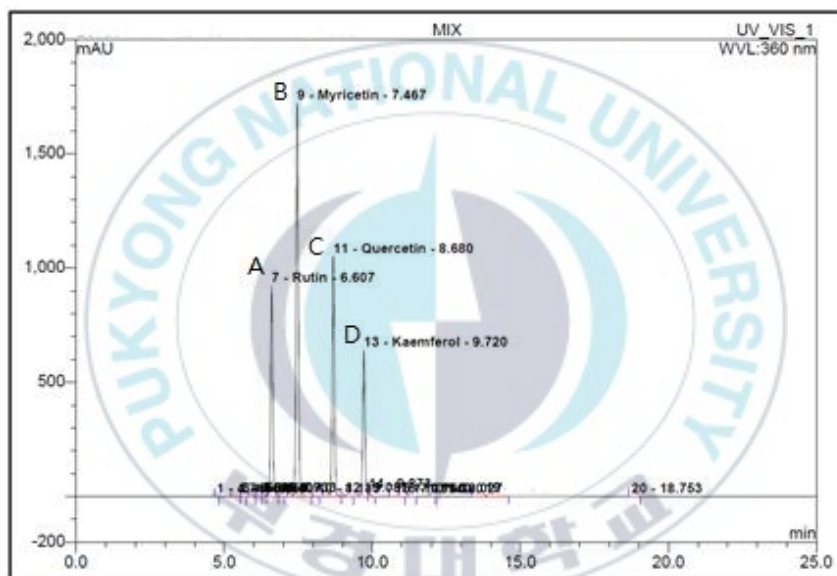
**Fig. 2.3. Standard peaks of the rutin (A), myricetin (B), quercetin (C),
and kaempferol (D).**

et al., 2018b). Although all conditions and species were not the same, these findings are similar to this study in that the content of flavonoids in tartary buckwheat sprouts grown in the light was higher than in the dark conditions. The findings indicated that light irradiation during germination affected the rutin content.

The contents of the myricetin, quercetin, and kaempferol flavonoids are presented in Fig. 2.5. Myricetin content displayed a similar tendency of rutin. It increased up to 6,000 lux, reaching 37.37 mg/L. Quercetin content also increased as the light intensity increased, with 62.73 mg/mL at 6,000 lux. Kaempferol content did not change significantly as light strength increased. However, kaempferol content was also highest at 6,000 lux. Kaempferol content ranged from 16.85 mg/L to 18.87 mg/L. Several studies evaluated the relationship between light and bioactive compounds before and after germination. However, there has not been an examination of light strength and germination. The tartary buckwheat sprouts grown in different color light displayed greater content of vietxin, isoviexin, quercetin-3-O-robinobioside, and rutin than those grown in the dark (Nam et al., 2018a). In another study, pea seedlings grown in blue, red, and white light displayed more chlorophyll and carotene compared to
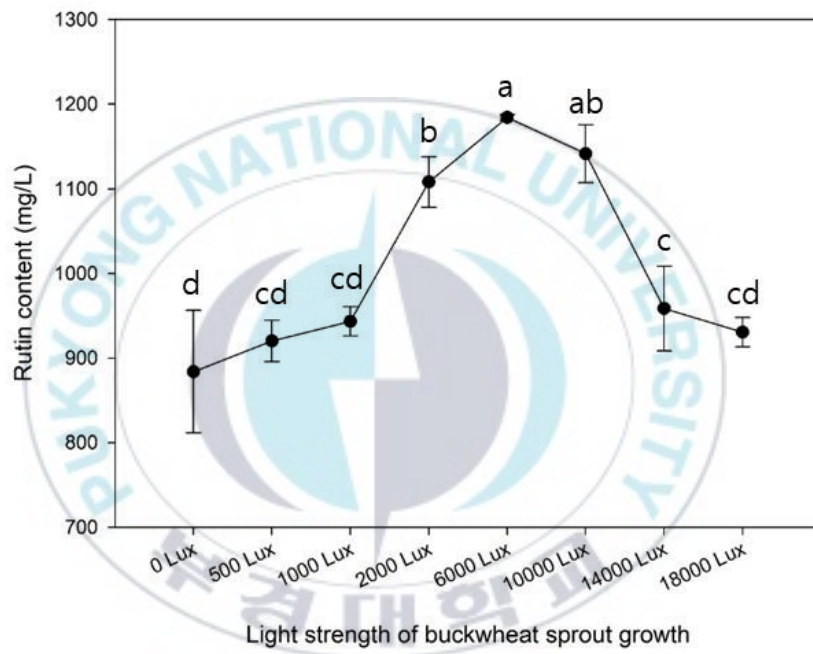
Fig. 2.4. Rutin content of tartary buckwheat sprouts grown using different light strengths.
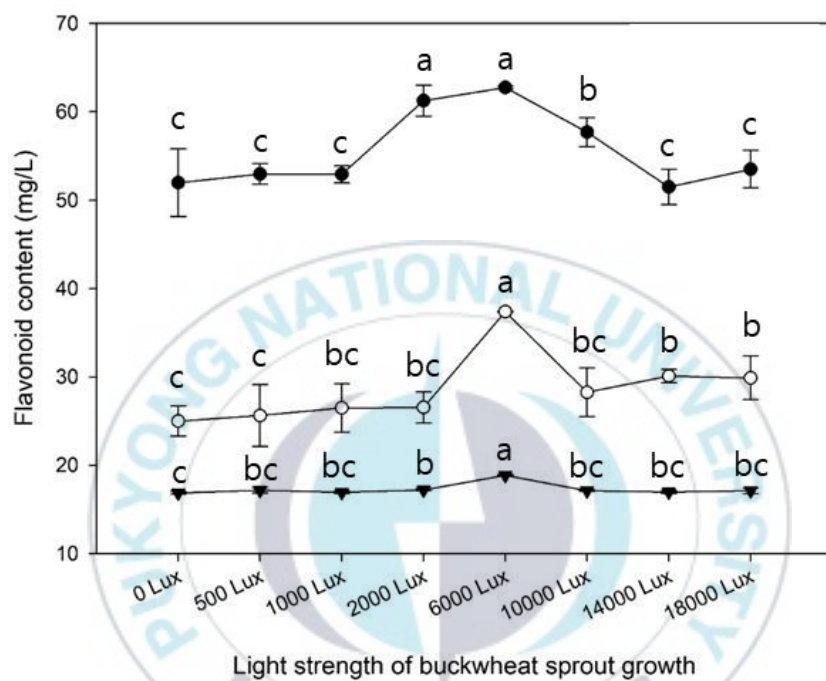
Fig. 2.5. Contents of myricetin, quercetin, and kaempferol flavonoids of tartary buckwheat sprouts grown under different highest strengths (▼,myricetin; ●, quercetin; ○ kaempferol).

seedlings grown in the dark (Wu et al., 2007). The prior results were similar to the presently observed increase in the bioactive compound. Since peas, common buckwheat, and tartary buckwheat showed similar tends, light irradiation may more generally enhance bioactive compounds.

2.3.3. Total polyphenol and flavonoid contents of tartary buckwheat sprouts grown at different light strengths

The total polyphenol contents of tartary buckwheat sprouts grown at different light strengths were displayed in Fig. 2.6. Total polyphenol content was increased for light intensities up to 10,000 lux. The highest total polyphenol content of tartary buckwheat sprouts was from those grown at 10,000 lux (1,213.04 mg/L), unlike rutin and other flavonoid content. Thereafter, the content decreased. However, there was no significant difference between 6,000 lux and 10,000 lux. In the case of common buckwheat germinated using different colored light and in the dark, the total polyphenol content in samples grown in the dark displayed the lowest content. Sprouts grown in blue light displayed the highest value of 84.9 mg GAE/g DW. Sprouts grown in red and white light displayed a higher content than those grown in the dark (Nam et al., 2018a).
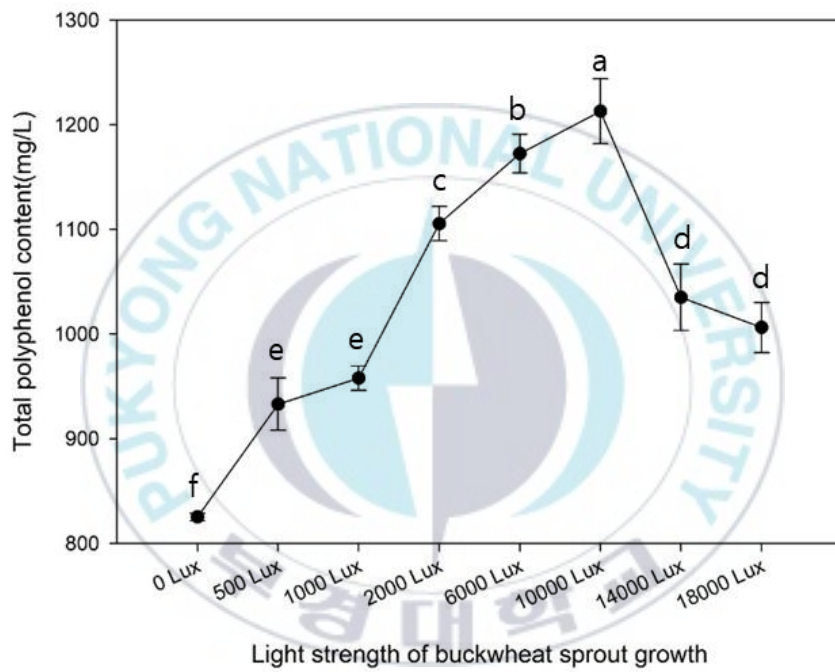
Fig. 2.6. Total polyphenol contents of tartary buckwheat sprouts grown in different light strengths.
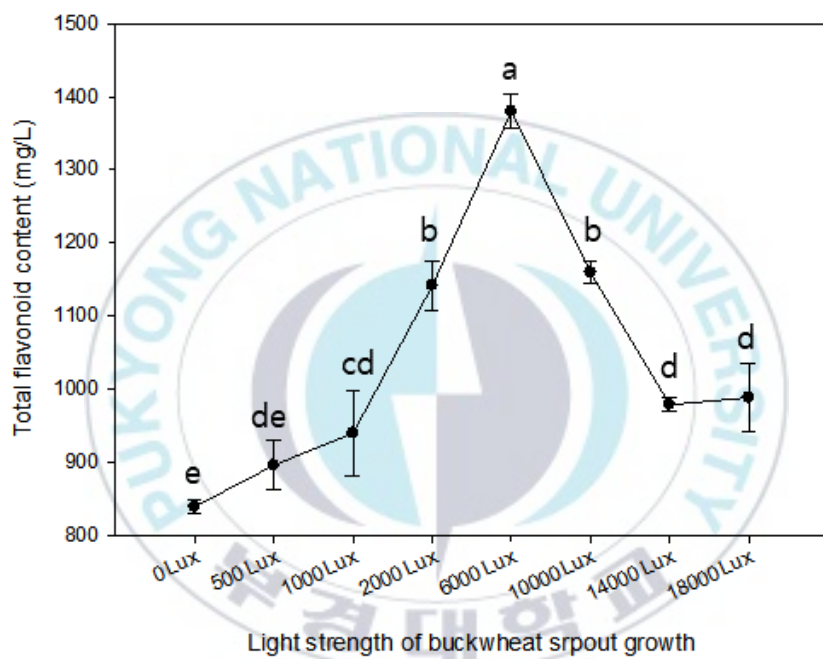
Fig. 2.7. Total flavonoid contents of tartary buckwheat sprouts grown in different light strengths.

Total flavonoid content was similar to the contents of rutin and other flavonoids as analyzed by HPLC (Fig. 2.7). The flavonoid content of tartary buckwheat sprouts grown at 0 and 6,000 lux was 838.82 and 1379.79 mg/L, respectively. Similar to the HPLC analysis result, the flavonoid content at 6,000 lux was the highest. According to Nam et al. (2018a), the total flavonoid content of common buckwheat grown in blue light was highest. Common buckwheat sprouts grown in the dark displayed significantly lower flavonoid contents than in the light (Nam et al., 2018a). Although comparisons could not be made under the same conditions, the flavonoid content in the dark was significantly lower than in sprout grown in the light. The findings implied that the light strength was related to the content of polyphenols and flavonoids. Furthermore, total polyphenol and flavonoid contents were increased during the aging black garlic and manufacturing process. The total flavonoids and polyphenol contents increased because they were converted to a form that eluted easily (Shin et al., 2008). One reason for the increase in the contents of total flavonoids and polyphenols is that they eluted more easily from sprouts than from grains.

2.3.4. Antioxidant activity of tartary buckwheat sprouts grown in different light strengths

The results of DPPH and ABTS radical scavenging activity assays were shown in Fig. 2.6. DPPH and ABTS radical scavenging activity showed different patterns. DPPH radical scavenging activity tended to increase and decrease similar to total polyphenol content. In addition, ABTS radical scavenging activity increased and decreased similar to total flavonoid contents. DPPH radical scavenging activity was highest (50.96 ± 0.60%) in extracts from buckwheat sprouts grown using 10,000 lux. ABTS radical scavenging activity was 30.69 ± 0.98% at 10,000 lux. Both DPPH and ABTS increased, with the highest activity at 10,000 lux. As mentioned in section 2.3.3., total polyphenol and flavonoid contents increased during manufacture and the aging of black garlic. Antioxidant activity was also increased in both DPPH and ABTS radical scavenging activities (Shin et al., 2008). Likewise, DPPH and ABTS radical scavenging activities followed the total flavonoid and polyphenol contents. FRAP activity also followed the pattern of total flavonoid contents. Sprouts grown using 6,000 lux light displayed the highest ferric reducing antioxidant activity (1.18 ± 0.09 μmol FeSO₄/mL), with the same tendency
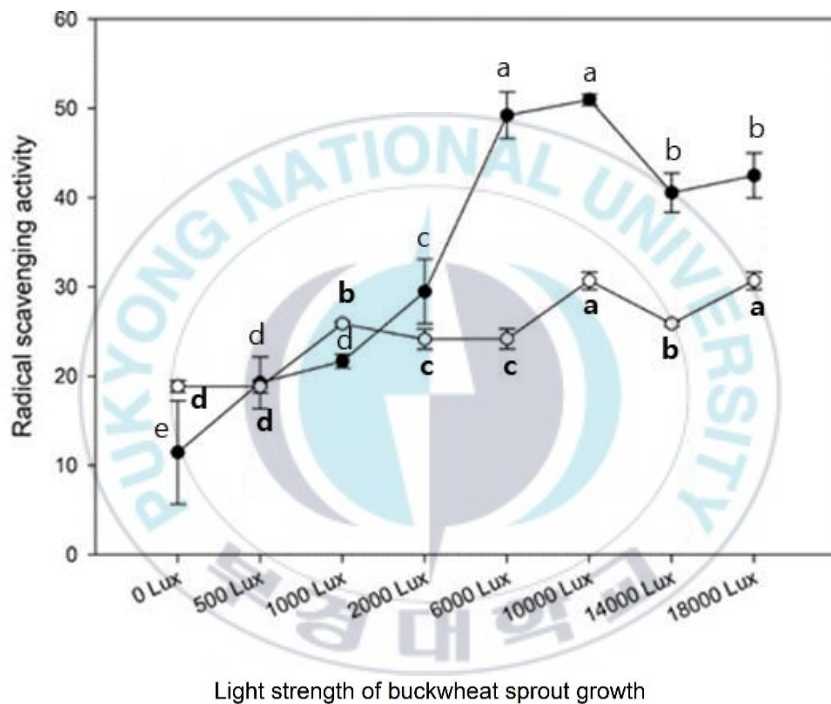
Fig. 2.8. Antioxidant activity (DPPH, ABTS radical scavenging activity) of tartary buckwheat sprouts grown in different light strengths (—●—, DPPH; —○—, ABTS)
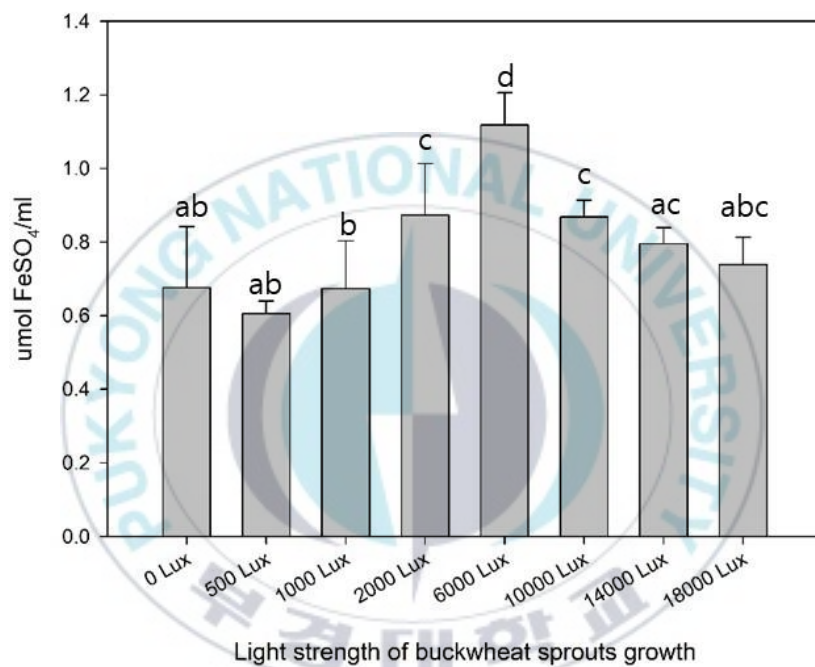
Fig. 2.9. Antioxidant activity (FRAP) of tartary buckwheat sprouts grown in different light strengths.

as the flavonoid contents. A study that measured the antioxidant activities of DPPH and ABTS radical scavenging activities and FRAP reported that stems, roots, and leaves showed a similar tendency in all antioxidant activities during tartary buckwheat growth (Ren et al., 2018). The antioxidant activity of sprouts grown in the light was higher than in the dark (Nam et al., 2018a). The antioxidant activities in this study had a similar tendency to those of previous studies.

2.3.5. Anti-hyperglycemic activity of tartary buckwheat sprouts grown in different light strengths

Diabetes is a metabolic disease that features an insufficient secretion of insulin and is characterized by high blood glucose levels. Therefore, it is crucial to control blood glucose levels in the treatment of diabetes. Two enzymes enhance the level of blood glucose: α-glucosidase and α-amylase. These enzymes are essential in carbohydrate digestion and produce glucose. Inhibition of those enzymes can control blood glucose levels. The results of α-glucosidase and α-amylase inhibitory activity, which could explain the anti-hyperglycemic activity, are displayed in Fig. 2.10 and 2.11. Both α-glucosidase and α-amylase inhibitory activity displayed the
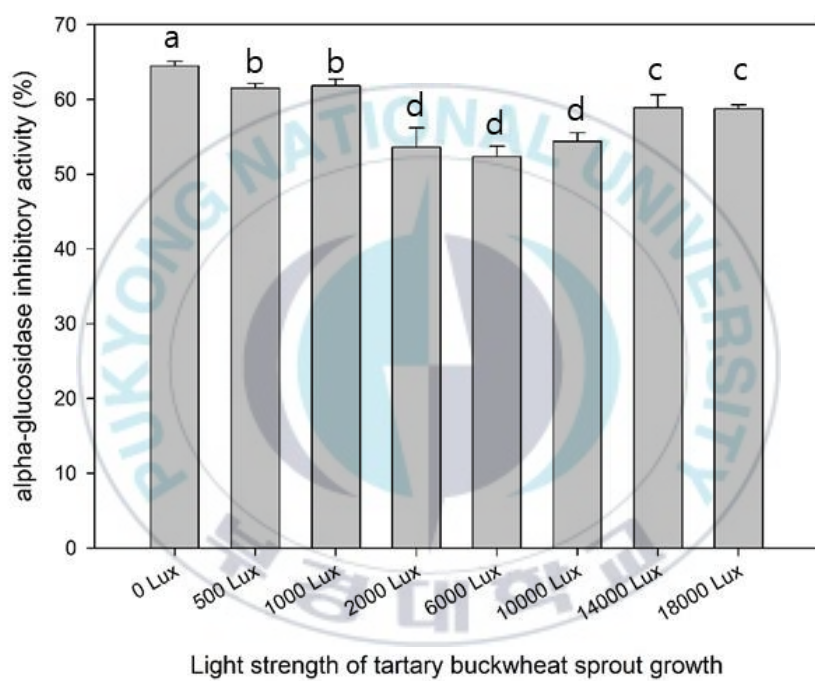
Fig. 2.10. α-Glucosidase inhibitory activity of tartary buckwheat sprouts grown in different light strengths.
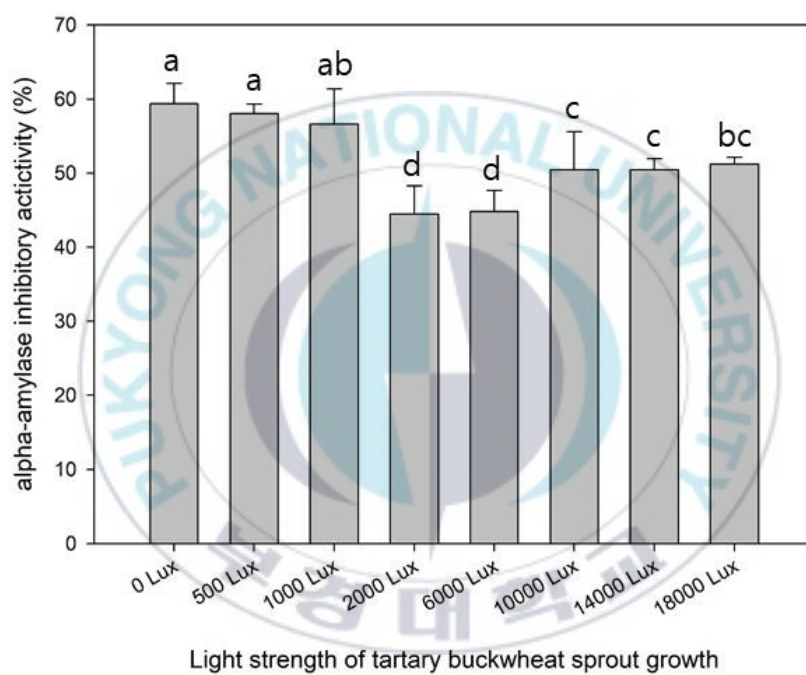
Fig. 2.11. α-Amylase inhibitory activity of tartary buckwheat sprouts grown in different light strengths.

same tendency. The α-glucosidase inhibitory activity of $52.37 \pm 1.36\%$ was the lowest and was obtained with tartary buckwheat sprouts grown at 6,000 lux. α-Amylase inhibitory activity was the lowest in sprouts grown at 2,000 and 6,000 lux (44.48 ± 3.76 and $44.82 \pm 2.84\%$, respectively). Both anti-hyperglycemic activities displayed opposite patterns from the flavonoid contents and antioxidant activities. Contrary to this study, other studies reported that flavonoids inhibited α-glucosidase (Feng et al., 2017; Tedera et al., 2006). However, another research reported that α-glucosidase inhibitory activity was affected by the root part of tartary buckwheat. The authors evaluated α-glucosidase inhibitory activity during tartary buckwheat growth, α-glucosidase inhibitory activity was increased with growth. Because there was no change in the stems and leaves, it was judged that root components, such as polysaccharides, inhibited the enzyme activity, with flavonoids, especially rutin, not being related to enzyme inhibition (Ren et al., 2018). Furthermore, α-glucosidase inhibitory activity was not increased as rutin content increased compared with other substances from *Lithocarpus polystachyus*. The activity was maintained a steady state at a rutin content exceeding 0.8 mg/mL, unlike the antioxidant activity (Dong et al., 2012). The findings indicated that

different components of the sprouts could inhibit enzymes related to the anti-hyperglycemic activity.

2.3.6. HMG-CoA reductase inhibitory activity of tartary buckwheat sprouts grown at different light strengths

3-Hydroxy-3-methylglutaryl-coenzyme A (HMG-CoA) reductase is the rate-limiting enzyme controlling cholesterol biosynthesis. Drugs that treat hypercholesterolemia mainly target this enzyme to control cholesterol (Vaughan et al., 2000). HMG-CoA is converted to mevalonate by this enzyme. When HMG-CoA reductase is inhibited, it effectively lowered the cholesterol level in almost all animals. Fig. 2.12 depicts the total flavonoid contents of tartary buckwheat sprouts grown in different light strengths. The assay kit was designed to detect HMG-CoA reductase inhibitory activity by measuring the oxidation of NADPH by the catalytic subunit of HMG-CoA reductase in the presence of the substrate HMG-CoA. The HMG-CoA reductase inhibitory activity displayed a different aspect of antioxidant activity. While the antioxidant activity increased with increasing light strengths, the HMG-CoA reductase inhibitory activity contrarily decreased as the light strength increased. The level of
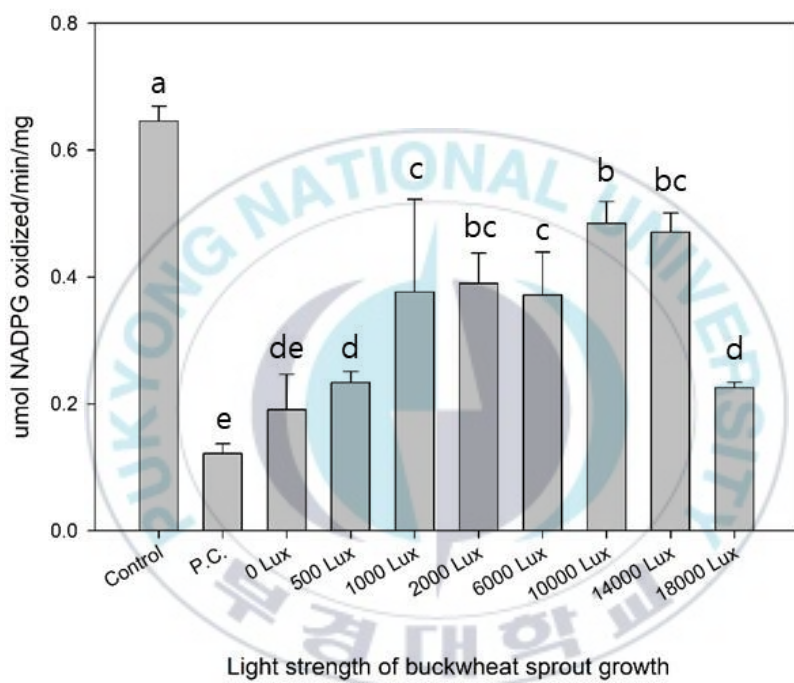
Fig. 2.12. HMG reductase inhibitory activity of tartary buckwheat sprouts grown in different light strengths.

58

the pravastatin positive control was 0.12 μmol oxidized/min/mg, which represented 81.13% of HMG-CoA reductase inhibitory activity. In addition, HMG reductase inhibitory activity was highest in sprouts grown in the dark, which was 70.44%, which was close to the pravastatin. The HMG-CoA reductase inhibitory activity was similar to the anti-glycemic activity. Both enzyme inhibitory activities displayed a different tendency of antioxidant activity. Another research reported that 10 μg/mL of rutin, kaempferol, quercetin, and rutin did not affect HMG-CoA reductase inhibitory activities of flavonoid compounds, did not show the activity. Some flavonoids, including morin and sophoraflavanone G, displayed activity. Most flavonoids did not have HMG-CoA reductase inhibitory activities (Son et al., 2018). In an animal experiment, tartary buckwheat flavonoids could reduce triglyceride and cholesterol levels in hyperlipidemic mice (Kuwabara et al., 2007; Ruan et al., 2020). The synthesis of cholesterol biosynthesis is complicated, which makes it difficult to judge that the results from the animal experiments were related to HMG-CoA reductase inhibitory activity. The pravastatin positive control was a competitive, reversible inhibitor that interacts with the binding site of the enzyme. That prevents the substrate from binding the

enzyme by a steric mechanism (Soares et al., 2015). The findings indicate that the enzyme inhibitory activity was derived from other compounds, such as amino acids and organic acids, except for the flavonoids.

2.3.7. The yield of tartary buckwheat sprouts grown using the smart farm system

In the first germination trial using the smart farm system, 1 kg of tartary buckwheat was used. After ten days of germination, the yield of tartary buckwheat sprouts was approximately 8.27 kg. Tartary buckwheat sprouts grew by up to 8.27 times by weight compared to tartary buckwheat grain. However, contaminating fungi were found in the roots, which rendered the roots unsuitable as food. The dark brown portion in Fig. 2.13 represents fungi. The cause of the contamination was likely starch from non-germinated tartary buckwheat and the residual water that was delayed in exiting the germination plate.

In the second trial, the germination condition in the smart farm was controlled to prevent fungi. The first method was to reduce the density of the tartary buckwheat to reduce non-germinated grains. It was confirmed

Fig. 2.13. Fungi produced on day 10 of the growth of sprout roots.

in a previous study that tartary buckwheat with insufficient air could not germinate. A smaller amount of tartary buckwheat was inoculated in one plate. The second method was to adjust the gradient of the plate for sprayed water to reduce contamination more conveniently. The third method, which applied to germination, was to add chlorine to the sprayed water to prevent fungi and harmful microorganisms during germination and growth of sprouts. The data of the yield of sprouts is shown in Table 2.3. Condition 1 (400 g of tartary buckwheat, 5° slope, no chlorine sterilization) displayed the highest yield. As the amount of tartary buckwheat was increased, the yield decreased. The finding indicated that the density of tartary buckwheat was vital for the germination. However, condition 1 was not suitable for productivity. The slope of the plate did not affect the yield.

Chlorine sterilization negatively affected the yield. Sprout production using 400 g of tartary buckwheat was 4,505 g. A 600 g quantity of tartary buckwheat yielded 6,612 g of sprouts. Considering yield and productivity, condition 3 was the best for the mass production of tartary buckwheat sprouts using the smart farm system. The germination rate of beet seeds that were sterilized with hydrogen peroxide and soaked in hydrogen

Table 2.3. Yield of buckwheat sprout compared with grain

	Mean weight of buckwheat sprouts (g)	Yield (%)
1	4,505	1,126
2	4,486	1,121
3	6,612	1,102
4	6,555	1,093
5	5,488	914
6	4,394	732
7	6,096	762
8	5,568	696

chloride was not affected (Lee et al., 2004). The findings indicated that germination conditions need to be adjusted according to the sprouts to be manufactured. In case of tartary buckwheat, chlorine sterilization did not need during the germination.

2.3.8. Flavonoid content of each germination plate in the smart farm system

The flavonoid content of each germination plate under the different conditions was shown in Fig. 2. 14. There was no significant difference in the content of the rutin, quercetin, and kaempferol flavonoids. The rutin, quercetin, and kaempferol content ranged from 593.92 to 603.74 mg/L, 236.51 to 253.37 mg/L, and 40.70 to 48.76 mg/L, respectively. However, myricetin was not detected. These conditions for germination in the smart farm system did not affect the second metabolites of the plants, such as flavonoids.

2.4. Conclusion

To evaluating the relationship between light strength and bioactive
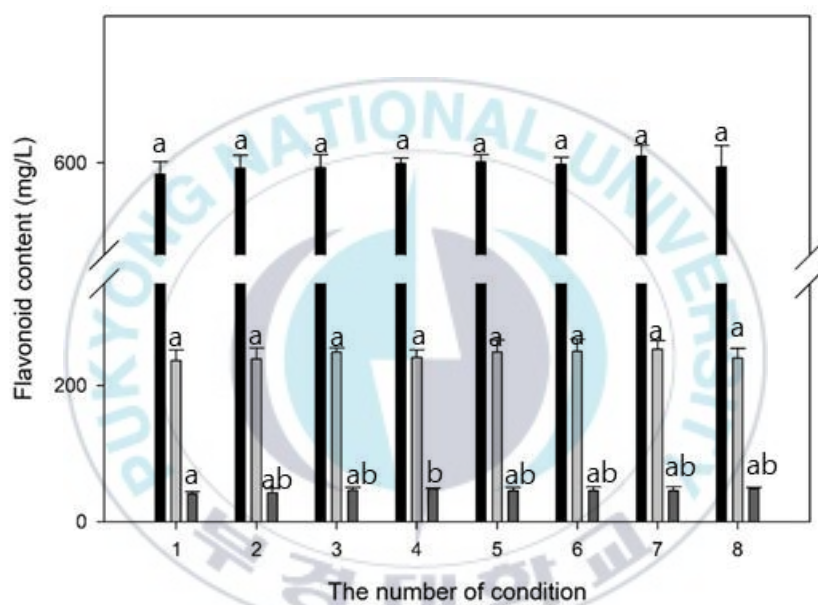
Fig. 2.14. Flavonoid content of each germination plate under different condition (rutin, ▬▬ ; quercetin, ▭▭ ; myricetin; ▬▬).

compound of tartary buckwheat sprouts, sprouts were germinated and grown in different light strengths. As the light intensity increased, the sprout color became progressively darker and redder. Rutin and other flavonoid contents in sprouts increased as the light intensity increased to 6,000 lux but decreased at intensities over 6,000 lux. However, kaempferol content was not significantly changed. However, total polyphenol displayed the highest content in sprouts grown at 8,000 lux. DPPH activity displayed a similar tendency to flavonoid content, and ABTS activity was similar to polyphenol content. The collective findings indicate that manufacturing tartary buckwheat sprouts using a light intensity of 6,000 lux was appropriate to enhance rutin content and antioxidant activity. Anti-glycemic and anti-cholesterol activities showed the opposite tendency. Thus, antioxidant activity appeared to depend on flavonoid and polyphenol contents and other activities related to enzyme inhibitory activities were dependent on other components.

Germination was needed to control variable conditions, such as water, humidity, light, and temperature. The smart farm system was suitable to grow sprouts. Therefore, for the commercial production of tartary buckwheat sprouts, the smart farm system and water culture were needed.

The optimal conditions of tartary buckwheat germination using a smart farm system involved control of the density of tartary buckwheat, slope of the plate, and the use of choline sterilization. The density of tartary buckwheat had the most effect on yield. Sprouts sterilized using chlorine displayed the lowest yield. The flavonoid content was not affected by these conditions. Thus, 600 g of tartary buckwheat per plate, 5° gradient, and lack of choline sterilization were determined as the optimal conditions considering yield and productivity.

2.5. References

Benzie IF, Strain JJ. 1996. The ferric reducing ability of plasma (FRAP) as a measure of "antioxidant power": the FRAP assay. Analytical Biochemistry, 239, 70-76.

Bonafaccia G, Marocchini M, Kreft I. 2003. Composition and technological properties of the flour and bran from common and tartary buckwheat. Food Chemistry, 80, 9-15.

Dong HQ, Li M, Zhu F, Liu FL, Huang JB. 2012. Inhibitory potential of trilobatin from Lithocarpus polystachyus Rehd against α-glucosidase and α-amylase linked to type 2 diabetes. Food Chemistry, 130, 261-

266.

Donkor ON, Stojanovska L, Ginn P, Ashton J, Vasiljevic T. 2012. Germinated grains–Sources of bioactive compounds. Food Chemistry, 135, 950-959.

Fabjan N, Rode J, Kosir IJ, Wang Z, Zhang Z, Kreft I. 2003. Tartary buckwheat (*Fagopyrum tataricum* Gaertn.) as a source of dietary rutin and quercitrin. Journal of Agricultural and Food Chemistry, 51, 6452-6455.

Feng L, Xie Y, Peng C, Liu Y, Wang H. 2018. A novel antidiabetic food produced via solid-state fermentation of tartary buckwheat by *L. plantarum* TK9 and *L. paracasei* TK1501. Food Technology and Biotechnology, 56, 373-380.

Gulpinar AR, Orhan IE, Kan A, Senol FS, Celik SA, Kartal M. 2012. Estimation of *in vitro* neuroprotective properties and quantification of rutin and fatty acids in buckwheat (*Fagopyrum esculentum* Moench) cultivated in Turkey. Food Research International, 46, 536-543.

Kim EO, Lee KT, Choi SW. 2008. Chemical comparison of germinated- and ungerminated-safflower (*Carthamus tinctorius*) seeds. Journal of

the Korean Society of Food Science and Nutrition, 37, 1162-1167.

Kuwabara T, Han KH, Hashimoto N, Yamauchi H, Shimada KI, Sekikawa M, Fukushima M. 2007. Tartary buckwheat sprout powder lowers plasma cholesterol level in rats. Journal of Nutritional Science and Vitaminology, 53, 501-507.

Lee JS, Pill WG, Cobb BB, Olszewski M. 2004. Seed treatments to advance greenhouse establishment of beet and chard microgreens. The Journal of Horticultural Science and Biotechnology, 79, 565-570.

Mendieta A, Jimenez F, Garduno-Siciliano L, Mojica-Villegas A, Rosales-Acosta B, Villa-Tanaca L, Montiel LE. 2014. Synthesis and highly potent hypolipidemic activity of alpha-asarone-and fibrate-based 2-acyl and 2-alkyl phenols as HMG-CoA reductase inhibitors. Bioorganic and Medicinal Chemistry, 22, 5871-5882.

Moongngarm A, Saetung N. 2010. Comparison of chemical compositions and bioactive compounds of germinated rough rice and brown rice. Food Chemistry, 122, 782-788.

Murphy CJ, Llort KF, Pill WG. 2010. Factors affecting the growth of microgreen table beet. International Journal of Vegetable Science, 16,

253-266.

Nam TG, Lim YJ, Eom SH 2018a. Flavonoid accumulation in common buckwheat (*Fagopyrum esculentum*) sprout tissues in response to light. Horticulture, Environment, and Biotechnology, 59, 19-27.

Nam TG, Kim DO, Eom SH. 2018b. Effects of light sources on major flavonoids and antioxidant activity in common buckwheat sprouts. Food science and biotechnology, 27, 169-176.

Qin P, Wu L, Yao Y, Ren G. 2013. Changes in phytochemical compositions, antioxidant and α-glucosidase inhibitory activities during the processing of tartary buckwheat tea. Food Research International, 50, 562-567.

Ren Q, Liu W, Zhao M, Sai CM, Wang JA. 2018. Changes in α-glucosidase inhibition, antioxidant, and phytochemical profiles during the growth of Tartary buckwheat (*Fagopyrum tataricum* Gaertn). International Journal of Food Properties, 21, 2689-2699.

Ruan J, Zhou Y, Yan J, Zhou M, Woo SH, Weng W, Zhang K. 2020. Tartary buckwheat: an under-utilized edible and medicinal herb for food and nutritional security. Food Reviews International, pp1-15.

Sheliya MA, Rayhana B, Ali A, Pillai KK, Aeri V, Sharma M, Mir SR.

2015. Inhibition of α-glucosidase by new prenylated flavonoids from *Euphorbia hirta* L. herb. Journal of Ethnopharmacology, 176, 1-8.

Shin JH, Choi DJ, Lee SJ, Cha JY, Kim JG, Sung NJ. 2008. Changes of physicochemical components and antioxidant activity of garlic during its processing. Journal of Life Science, 18, 1123-1131.

Soares RAM, Mendonca S, De Castro LIA, Menezes ACCCC, Areas JAG. 2015. Major peptides from amaranth (*Amaranthus cruentus*) protein inhibit HMG-CoA reductase activity. International Journal of Molecular Sciences, 16, 4150-4160.

Son KH, Lee JY, Lee JS, Kang SS, Sohn HY, Kwon CS. 2018. Screening of flavonoid compounds with HMG-CoA reductase inhibitory activities. Journal of Life Science, 28, 247-256.

Tadera K, Minami Y, Takamatsu K, Matsuoka T. 2006. Inhibition of α-glucosidase and α-amylase by flavonoids. Journal of Nutritional Science and Vitaminology, 52, 149-153.

Thaipong K, Boonprakob U, Crosby K, Cisneros-Zevallos L, Byrne DH. 2006. Comparison of ABTS, DPPH, FRAP, and ORAC assays for estimating antioxidant activity from guava fruit extracts. Journal of Food Composition and Analysis, 19, 669-675.

Vaughan CJ, Gotto AM, Basson CT. 2000. The evolving role of statins in the management of atherosclerosis. Journal of the American College of Cardiology, 35, 1-10.

Waterland NL, Moon Y, Tou JC, Kim MJ, Pena-Yewtukhiw EM, Park S. 2017. Mineral content differs among microgreen, baby leaf, and adult stages in three cultivars of kale. Hort Science, 52, 566-571.

Wu MC, Hou CY, Jiang CM, Wang YT, Wang, CY, Chen HH, Chang HM. 2007. A novel approach of LED light radiation improves the antioxidant activity of pea seedlings. Food Chemistry, 101, 1753-1758.

Yoon BR, Cho BJ, Lee HK, Kim DJ, Rhee SK, Hong HD, Lee OH. 2012. Antioxidant and anti-adipogenic effects of ethanolic extracts from tartary and common buckwheats. Korean Journal of Food Preservation, 19, 123-130.

Zhang ZL, Zhou ML, Tang Y, Li FL, Tang YX, Shao JR, Wu YM. 2012. Bioactive compounds in functional buckwheat food. Food Research International, 49, 389-395.

Chapter 3. Optimization of flavonoid extraction conditions from tartary buckwheat sprout using response surface methodology

Abstract

In this study, the purpose was to optimize the extraction conditions of rutin, quercetin, and myricetin flavonoids from tartary buckwheat sprouts using response surface methodology (RSM). A Box-Behnken design containing 15 experiments was employed to evaluate the effect of temperature (X_1, 50-70°C), extraction time (X_2, 5-9 h), and ethanol concentration (X_3, 60-90%). The models of each flavonoid were accurate in predicting the optimal extraction conditions. The optimal extraction conditions that maximized rutin, quercetin, and myricetin contents were X_1=51.03, X_2=6.62, and X_3=69.16%. At these conditions, the predicted rutin, quercetin, and myricetin contents were 808.467, 193.296, and 37.360 μg/mL, respectively.

3.1. Introduction

Buckwheat is an annual plant in the Polygonaceae family. It is a crop that grows in a cool and humid climate (Przybylsk et al., 1998). Buckwheat was purported to have effects on mental clarity and helps remove waste generally in the body. It has been recommended as an addition to food for patients with high blood pressure or vascular system problems, such as arteriosclerosis. In general, bioactive substances are enriched in tartary buckwheat compared to general buckwheat. There are abundant polyphenols, including six flavonoids in tartary buckwheat. Important flavonoids in buckwheat include rutin, orientin, quercetin, vitexin, isovitexin, and isoorientin (Fabjan et al., 2003; Kang, 2015; Liu et al., 2008; Zhang et al., 2012).

Rutin, also termed sophrin, is a combination of quercetin and rutinose (a disaccharide of rhamnose and glucose, also termed quercetin-3-rutinoside). Pure rutin is yellow to pale yellow in color. Rutin is the best-known flavonoid in buckwheat due to its antioxidant, anti-inflammatory, and anti-cancer properties (Chua, 2013; Kang, 2015). Rutin also protects against hepatocyte damage caused by gamma irradiation, controls blood vessel permeability, and strengthens capillaries (Kang, 2015; Kwon, 1994;

Kreft et al.,2006). Rutin has been used as a raw material for more than 130 pharmaceuticals and in the food and beverage industries.

Quercetin (3, 3', 4', 5, 7-pentahydroxyflavone) is a physiologically active substance found in fruits and vegetables. Benefits attributed to quercetin include anti-inflammatory, anti-cancer, and anti-viral activities and protection of heart function and the nervous system (Boots et al., 2007; Davis et al., 2009; Harwood et al., 2007; Utesch et al., 2008). Quercetin also is involved in intracellular mitochondria biosynthesis (Aguirre et al., 2011). Finally, quercetin may improve physical ability and provide mental stimulation similar to caffeine (Davis et al., 2003).

Myricetin (3, 3', 4', 5, 5', 7-hexahydroxyflavone) is also widespread in plants, such as tea, berries, fruits, and vegetables. It has been unequivocally demonstrated that myricetin is related to antioxidant activity. Myricetin has excellent enzymatic and non-enzymatic mechanisms to remove radicals (Ong et al., 1997). Myricetin can act as a prooxidant and thus can cause oxidative stress-related damage. However, prooxidants act differently depending on the surrounding environment (Carocho et al., 2013; Chobot et al., 2011). Additionally, myricetin can reportedly reduce the risk of skin cancer caused by polycyclic aromatic

hydrocarbons and also the origin and development of skin cancer (Mukhtar et al., 1988).

In this study, tartary buckwheat sprouts were grown and the flavonoids were extracted. The rutin, quercetin, and myricetin flavonoids, which are functional substances, were maximally extracted using conditions that were optimized using RSM.

3.2. Materials and methods

3.2.1. Materials

Tartary buckwheat was grown on Jeju Island. The material was used to manufacture tartary buckwheat sprouts was followed. In this process, the buckwheat was immersed in water at room temperature for 24 h, the water was removed, and germination of the buckwheat occurred in the dark conditions for 24 h in a model JSPC-420C plant growth chamber (JS Research Inc., Gongju, Republic of Korea). During the growth of sprouts, the buckwheat retained moisture so that complete immersion in water was not required. After 8 days of growth, the sprouts were harvested by removing the roots. The roots were dried for 24 h at 40°C using a hot air dryer. The dried material stored at -20°C until required.

76

Rutin (3,3′,4′,5,7-pentahydroxyflavone 3-rutinoside), quercetin (2-(3,4-dihydroxyphenyl)-3,5,7-trihydroxy-4H-1-benzopyran-4-one), and myricetin (3,3′,4′,5,5′,7-Hhexahydroxyflavone) were purchased from Sigma-Aldrich Co. (St. Louis, MO, USA). Methanol and water for HPLC were purchased from J.T. Baker (Phillipsburg, NJ, USA).

3.2.2. Ethanol extraction of tartary buckwheat sprouts

To extract tartary buckwheat sprouts, 1 g of dried tartary buckwheat sprouts was suspended in 20 mL ethanol in a 50 mL conical tube. The tube was immersed in a constant-temperature water tank with shaking at 130 rpm. The extracts were filtered through No. 3 quantitative filter paper (Adventec, Tokyo, Japan). The filtrate was stored and used for the experiment.

3.2.3. Design of extraction optimization

The preliminary experiment used various conditions that included extraction temperature (40, 50, 60, 70, 80, 90°C), extraction time (3, 4, 5, 6, 7, 8, 9 h), ethanol concentration (50, 60, 70, 80, 90%), and ratio of sample and solvent (1:5, 1:10, 1:15, 1:20).

To optimize the extraction conditions of tartary buckwheat sprout, RSM was used. Three different independent variables were selected using a Box-Behnken design that involved extraction temperature (X_1, 40-60℃), extraction time (X_2, 3-7 h), and concentration of the ethanol solvent (X_3, 50-90%) with three levels of each variable. The Box-Behnken design involved 15 experiments in Table 3.1. The order of experiments was randomized, and the runs were carried out in a single block.

3.2.4. Analysis of flavonoid content using HPLC

Flavonoid content was analyzed by HPLC using a model U-3000 device (Thermo Fisher Scientific Inc., Waltham, MA, USA). Before the analysis, all samples were filtered through a 0.45 μm cellulose acetate syringe filter (DISMIC-13cp; Toyo Roshi Kaisha, Ltd, Tokyo, Japan). The analysis column was an Acclaim C18 column (250×4.6 mm, 5 μm; Thermo Fisher Scientific Inc.). The mobile phases were 0.03 M phosphoric acid (A) and methanol (B). Elution was performed using the following gradient: 0 min, 60% A; 10 min 0% A; 15 min 0% A; 20 min 60% A; and 25 min 60% A. The flow rate was 1.0 mL/min and the detection wavelength was 360 nm. Flavonoids were quantified using

Table 3.1. Box-Behnken design and responses of dependent variables for optimization of extraction conditions considering three independent variables

Order	Independent variables			Responses		
	$X_1^{1)}$	X_2	X_3	Y_1	Y_2	Y_3
1	40(-1)	3(-1)	70(0)	627.53	138.42	27.21
2	60(+1)	3(-1)	70(0)	813.48	153.50	37.26
3	40(-1)	7(+1)	70(0)	751.30	195.77	33.27
4	60(+1)	7(+1)	70(0)	812.50	178.75	38.81
5	40(-1)	5(0)	50(-1)	735.46	156.04	31.40
6	60(+1)	5(0)	50(-1)	811.12	138.43	37.42
7	40(-1)	5(0)	90(+1)	665.44	169.54	22.26
8	60(+1)	5(0)	90(+1)	804.07	189.97	31.77
9	50(0)	3(-1)	50(-1)	707.57	153.81	29.05
10	50(0)	7(+1)	50(-1)	768.66	168.29	33.88
11	50(0)	3(-1)	90(+1)	713.92	187.90	20.22
12	50(0)	7(+1)	90(+1)	761.89	209.94	28.81
13	50(0)	5(0)	70(0)	782.20	180.67	36.69
14	50(0)	5(0)	70(0)	792.30	185.30	35.62
15	50(0)	5(0)	70(0)	785.90	190.92	35.07

[1] X_1, temperature (°C); X_2, time (h); X_3, ethanol concentration (%); Y_1, rutin content (μg/mL); Y_2, quercetin content (μg/mL); Y_3, myricetin content (μg/mL)

calibration curves of rutin, quercetin, and myricetin solutions (2.5-125 µg/mL) and the described analytical conditions.

3.2.5.　Verification of model

The optimal extraction temperature, time, and ethanol concentration conditions to maximize flavonoid contents from tartary buckwheat sprouts were determined by comparing actual experimental values with predicted values from the final response regression. The actual values were determined in ten repeat experiments.

3.2.6.　Statistical analysis

Design-Expert 7.0 software (Stat-Ease Inc., Minneapolis, MN, U.S.A) was used to obtain the optimal conditions through the analysis of experimental results. The independent variables X_i and X_j, and the response variable Y (contents of rutin, quercetin, myricetin) were fit into the following polynomial regression equation:

$$Y = \beta_0 + \sum_{i=1}^{k} \beta_i X_i + \sum_{i=1}^{k} \beta_{ii} X_i^2 + \sum_{i=1}^{k-1} \sum_{j>1}^{k} \beta_{ij} X_i X_j$$

80

where β_0 is a constant, β_i, β_{ii} and β_{ij} are linear, quadratic, and cross-product coefficients, respectively, X_i and X_j are the levels of the independent variables, k is the number of variables, and e is the random error of the model. ANOVA was used to determine the statistical significance, fit, lack of fit, and regression coefficient of the model. All experiments were repeated three times. A p-value ≤ 0.05 was statistically significant.

3.3. Results and discussion

3.3.1. Response surface analysis for flavonoid content

Determination of the contents of rutin, quercetin, and myricetin extracted from tartary buckwheat sprouts confirmed that each flavonoid increased as the extraction temperature increased. However, extraction was not performed properly because of ethanol evaporation at temperatures above 70°C. Comparison of the flavonoid contents revealed that each increased with time for up to 7 h, with a similar tendency as noted for temperature. However, flavonoid contents did not increase beyond 7 h and tended to maintain the same concentration. As a result, the temperature range was set at 40 to 60°C to prevent ethanol evaporation

and to extract effectively.

The extraction time range was set from 3 h, which was a relatively short time, to 7 h when the change in flavonoid content change was obvious. In addition, the ethanol concentration range was broad, from 50 to 90%. RSM to establish the optimal conditions to maximize rutin, quercetin, and myricetin contents, independent variables were determined as temperatures of 40 to 60℃, extraction times of 3 to 7 h, and ethanol concentrations of 50 to 90%.

Responses (experimental values) to optimize extraction conditions based on the Box-Behnken design considering three independent variables are shown in Table 3.1. The maximum values of rutin, quercetin, and myricetin were 813.48 μg/mL, 209.94 μg/mL, and 38.81 μg/mL, respectively. The respective minimum values were 627.53 μg/mL, 138.42 μg/mL, and 20.22 μg/mL. However, the minimum rutin and quercetin contents were evident following extraction at 40℃ for 3 h using 70% ethanol.

Coefficients of determination (R^2) of all the dependent variables (extraction temperature, extraction time, extraction ethanol concentration) exceeded 0.9 and were significant. The *p*-value of the model for lack of fit

was >0.1, indicating the predictive nature of the model.

3.3.2. Influence of extraction conditions on rutin content

The data of the RSM model of rutin content was validated by ANOVA of the response variables for the quadratic polynomial model are summarized in Table 3.2 and Fig. 3.1. The model was significant, as demonstrated by the F-value of 41.52, $p=0.0004$ ($p<0.05$), and R^2 of 0.9786. The p-value of the lack of fit test was 0.3332 ($p>0.01$), indicating the lack of significance. The collective values indicated that the model could predict the optimal extraction conditions.

The adjusted R^2 of 0.9401 indicated that the total change of 94.01% for the independent variables and the model could not explain only 5.99% of the total variation. The predictable R^2 of 0.6740 was not close to the adjusted R^2, as one might generally expect. The finding might indicate a large block effect or a possible problem with the model or data. According to ANOVA, the quadratic polynomial equation on rutin content, including three variables (temperature, time, ethanol concentration) is as follows:

Table 3.2. ANOVA for response surface quadratic model: regression model of the relationship between response variables and rutin

Source	Sum of Squares	df	Mean Square	F Value	p-value	Remark
Model	43255.27	9	4806.14	25.42	0.0012	significant
X_1	26615.71	1	26615.71	140.78	< 0.0001	
X_2	6718.91	1	6718.91	35.54	0.0019	
X_3	750.57	1	750.57	3.97	0.1029	
X_1X_2	3890.45	1	3890.45	20.58	0.0062	
X_1X_3	991.29	1	991.29	5.24	0.0707	
X_2X_3	43.02	1	43.02	0.23	0.6535	
X_1^2	354.18	1	354.18	1.87	0.2294	
X_2^2	2458.61	1	2458.61	13.00	0.0154	
X_3^2	1950.81	1	1950.81	10.32	0.0237	
Residual	945.32	5	189.06			
Lack of Fit	893.12	3	297.71	11.41	0.0817	not significant
Pure Error	52.20	2	26.10			
Cor Total	44200.59	14				

[1] X_1, temperature (℃); X_2, time (h); X_3, ethanol concentration (%); df, degrees of freedom

* R^2, 0.9786; Adj-R^2, 0.9401, Pred-R^2, 0.6740; Adq precision, 16.425

(A)

(B)

(C)

Fig. 3.1. Response surface plots for the effects of time, temperature, and ethanol concentration on rutin contents of extracts (A, time-temperature; B, ethanol concentration-temperature; C, ethanol concentration-time).

$$Y_1 = -370.89124 + 17.84889X_1 + 162.90749X_2 + 4.03506X_3 -$$

$$1.55934X_1X_2 + 0.078712X_1X_3 - 0.081988X_2X_3 - 0.097941X_1^2 -$$

$$6.45113X_2^2 - 0.057464X_3^2$$

Among the primary terms, extraction temperature (X_1) and time (X_2) were significant. Only extraction temperature and time (X_2X_3) were significant among the reciprocal terms. Time (X_2^2) and ethanol concentration (X_3^2) were significant secondary terms. There were no other terms that were significant. Another research reported that when rutin was extracted from Amaranth leaves under high pressure, the effect of the ratio of ethanol and water (i.e., the concentration of ethanol) was the greatest (Kraujalis et al., 2015). A similar tendency was evident in the present study.

3.3.3. Influence of extraction conditions on quercetin content

The RSM model of quercetin content was validated by ANOVA of the response variables for the quadratic polynomial model. The data are summarized in Table 3.3 and Fig. 3.2. The significance of the model was evident by the F-value of 40.81, $p=0.0102$ ($p<0.05$) and R^2 of 0.9478. In

Table 3.3. ANOVA for response surface quadratic model: regression model of the relationship between response variables and quercetin

Source	Sum of Squares	df	Mean Square	F Value	p-value	Remark
Model	6082.46	9	675.83	10.08	0.0102	significant
X_1	0.10	1	0.10	0.00	0.9712	
X_2	1773.73	1	1773.73	26.46	0.0036	
X_3	2477.06	1	2477.06	36.95	0.0017	
X_1X_2	257.84	1	257.84	3.85	0.1071	
X_1X_3	361.49	1	361.49	5.39	0.0679	
X_2X_3	14.27	1	14.27	0.21	0.6640	
X_1^2	1163.85	1	1163.85	17.36	0.0088	
X_2^2	5.90	1	5.90	0.09	0.7786	
X_3^2	70.83	1	70.83	1.06	0.3512	
Residual	335.23	5	67.05			
Lack of Fit	282.46	3	94.15	3.57	0.2266	not significant
Pure Error	52.77	2	26.38			
Cor Total	6417.69	14				

[1] X_1, temperature (°C); X_2, time (h); X_3, ethanol concentration (%); df, degrees of freedom

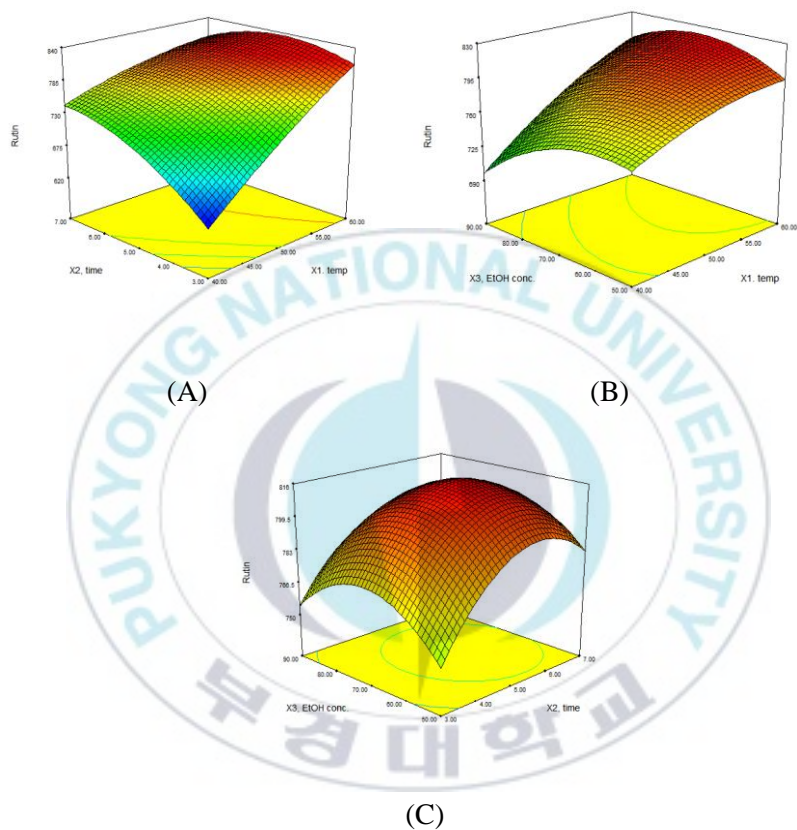* R^2, 0.9478; Adj-R^2, 0.8537, Pred-R^2, 0.2773; Adq precision, 11.646

Fig. 3.2. Response surface plots for the effects of time, temperature, and ethanol concentration on quercetin contents of extracts (A, time-temperature; B, ethanol concentration-temperature; C, ethanol concentration-time).

the lack of fit test, the *p*-value of 0.6643 exceeded 0.1, indicating a lack of significance. Thus, this RSM model could explain the change of quercetin content. The relationship between the response variable (quercetin content, Y_2) and the measured variable (extraction temperature, X_1; time, X_2; ethanol concentration, X_3) was a quadratic polynomial equation as below;

$$Y_2=-336.61147+16.44504X_1+27.37256X_2-0.19994X_3-$$
$$0.40144X_1X_2+0.047532X_1X_3+0.047215X_2X_3-0.17754X_1^2-$$
$$0.31608X_2^2-0.010949X_3^2$$

Among the primary terms, time (X_2) and ethanol concentration (X_3) were significant. The reciprocal terms of extraction temperature and time (X_1X_2) were significant. Of the double terms, only extraction temperature (X_1^2) was significant. Another research reported that when quercetin was extracted from onion skin, ethanol concentration, extraction time, and ultrasonic intensity did not significantly affect the quercetin content(Heo et al., 2019). Another study described that quercetin extraction from onion peels was not significantly affected by extraction time(Jang et al., 2012). However, this study observed that extraction time and ethanol concentration were the main factors affecting quercetin extraction from

89

tartary buckwheat sprouts. The difference between the prior and present results could reflect differences in the original materials.

3.3.4. Influence of extraction condition on myricetin content

The RSM model for myricetin content was validated by ANOVA of the response variables for the quadratic polynomial model. The data are summarized in Table 3.4 and Fig. 3.3. The significance of the model was evident by the F-value of 41.52, p-value of 0.0004 ($p<0.05$), and R^2 of 0.9868. In the lack of fit test, the p-value was 0.3332 ($p>0.1$), indicating the absence of significance. The collective findings indicated that the model could be sufficient to predict the change of myricetin. The relationship expressed as a response variable equation is:

$$Y_3=-37.369775-0.16749X_1+7.94953X_2+1.44983X_3-$$
$$0.056265X_1X_2+0.0043691X_1X_3+0.023575X_2X_3$$
$$+0.00531957X_1{}^2-0.54729X_2{}^2-0.014039X_3{}^2$$

In this model, all the independent variables, extraction temperature (X_1), time (X_2), and ethanol concentration (X_3), recognize to

Table 3.4. ANOVA for response surface quadratic model: regression model of the relationship between response variables and myricetin

Source	Sum of Squares	df	Mean Square	F Value	*p*-value	Remark
Model	423.10	9	47.01	41.52	0.0004	significant
X_1	121.04	1	121.04	106.89	0.0001	
X_2	55.22	1	55.22	48.76	0.0009	
X_3	102.84	1	102.84	90.81	0.0002	
X_1X_2	5.07	1	5.07	4.47	0.0881	
X_1X_3	3.05	1	3.05	2.70	0.1614	
X_2X_3	3.56	1	3.56	3.14	0.1365	
X_1^2	1.04	1	1.04	0.92	0.3809	
X_2^2	17.70	1	17.70	15.63	0.0108	
X_3^2	116.43	1	116.43	102.82	0.0002	
Residual	5.66	5	1.13			
Lack of Fit	4.32	3	1.44	2.15	0.3332	not significant
Pure Error	1.34	2	0.67			
Cor Total	428.76	14				

[1] X_1, temperature (℃); X_2, time (h); X_3, ethanol concentration (%); df, degrees of freedom

* R^2, 0.9868; Adj-R^2, 0.9630, Pred-R^2, 0.8317; Adq precision, 21.516
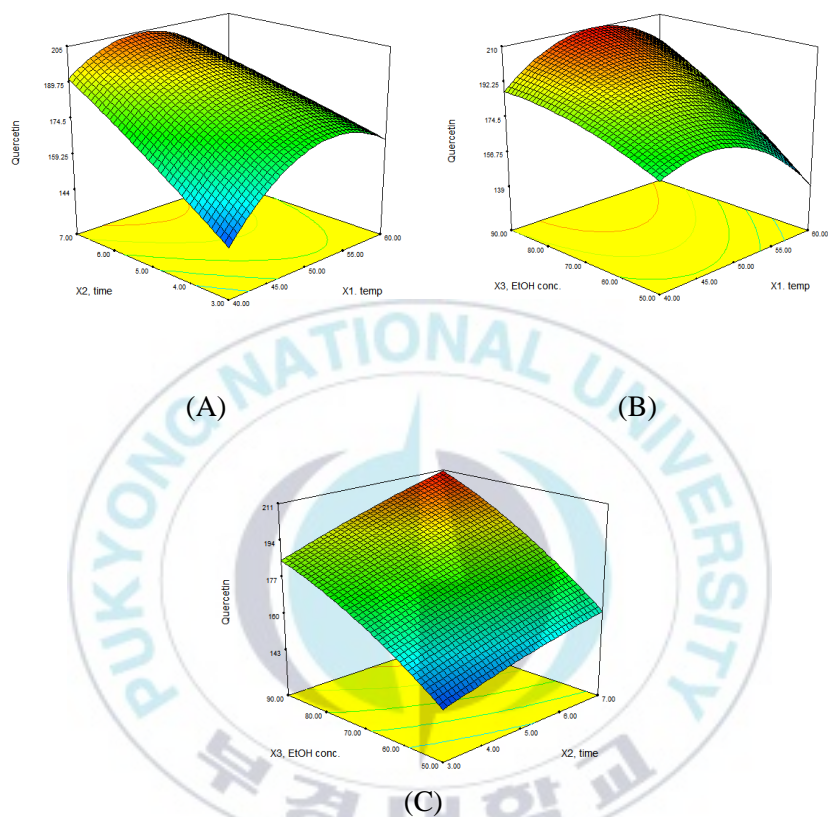
(A)

(B)

(C)
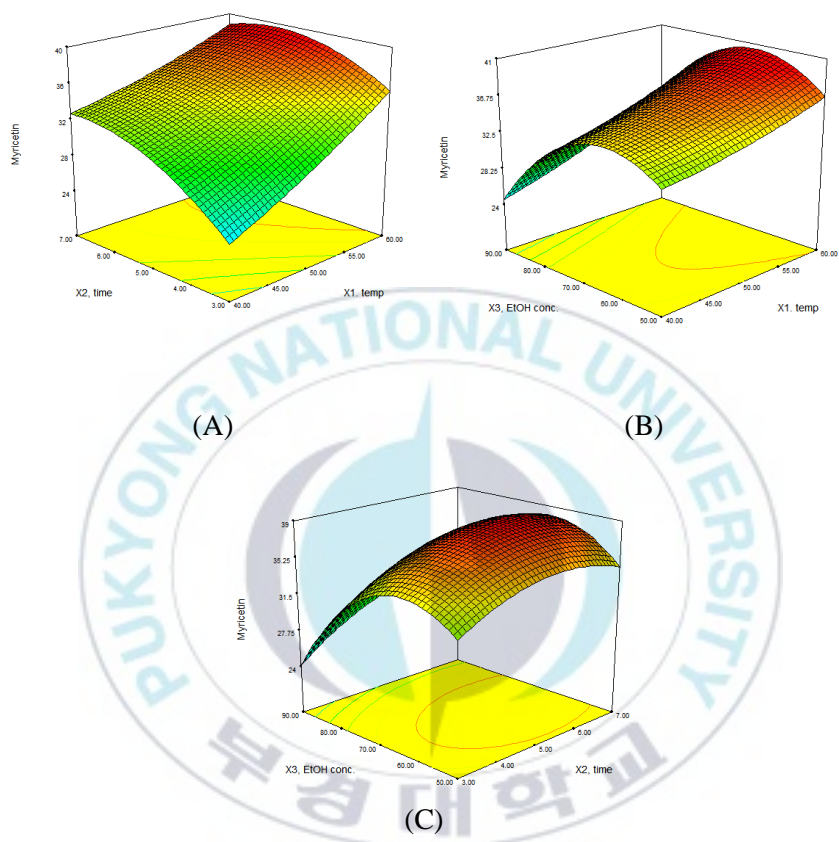
Fig. 3.3. Response surface plots for the effects of time, temperature, and ethanol concentration on myricetin contents of extracts (A, time-temperature; B, ethanol concentration-temperature; C, ethanol concentration-time).

(quercetin content, Y_2), and the measured variables (extraction temperature, X_1; time, X_2; and ethanol concentration, X_3) were quadratic polynomials that were significant primary terms. There was no significance of any reciprocal terms. In the double terms, extraction temperature (X_1^2) and ethanol concentration (X_3^2) were significant, while extraction temperature (X_2^2) was not.

3.3.5. Optimized conditions for maximizing rutin, quercetin, and myricetin contents

The optimization conditions and predicted values to maximize rutin, quercetin, and myricetin contents are summarized in Table 3.5. To maximize only rutin content as a single response, extraction using 66.07% ethanol for 5.22 h at 59.73°C was optimal. When extracted under these conditions, the rutin content was predicted to be 831.25 μg/mL. RSM analysis was performed to maximize the quercetin content as a single response. Optimal condition for rutin contents was determined to extract 90% of ethanol at 50.00°C for up to 7.00 h. The quercetin content was predicted to be 214.36 μg/mL. Extraction using 59.63% ethanol at 59.41°C

Table 3.5. Optimal extract conditions to maximize rutin, quercetin, and myricetin contents, and predicted rutin, quercetin, and myricetin content

Optimal condition		Predicted value	
Temperature (°C)	59.73	Rutin (μg/mL)	831.25
Time (h)	5.22		
Ethanol concentration (%)	66.07		
Temperature (°C)	5.00	Quercetin (μg/mL)	214.36
Time (h)	7.00		
Ethanol concentration (%)	90.00		
Temperature (°C)	59.41	Myricetin (μg/mL)	39.969
Time (h)	5.31		
Ethanol concentration (%)	59.63		

during 5.31 h was performed to maximize only myricetin content as a single response. When the myricetin was extracted from tartary buckwheat sprouts, its content was predicted to be 39.963 μg/mL.

The single response data determined that extraction performed using 75.04% ethanol at 55.23℃ for 6.37 h was optimal to simultaneously maximize rutin, quercetin, and myricetin (Table 3.6). The predicted rutin, quercetin, and myricetin content under the optimal conditions were 808.467 μg/mL, 193.296 μg/mL, and 37.3614 μg/mL, respectively.

3.3.6. Verification of the optimized condition for flavonoid contents

When the experiment was conducted under the conditions that were optimal for the maximum extraction of rutin, quercetin, and myricetin content, the predicted values were 808.467 μg/mL, 193.296 μg/mL, and 37.3614 μg/mL, respectively. To validate this model, ten repetitions of extraction from tartary buckwheat sprouts were performed. The actual content of rutin, quercetin, and myricetin was 802.84±8.49 μg/mL, 193.76±2.80 μg/mL, and 34.84±0.43 μg/mL, respectively.

Rutin content was lower than the predicted value. However, there

Table 3.6. Optimal extract conditions to maximize flavonoid content

and predicted flavonoid content

Optimal condition		Predicted value	
Temperature (°C)	55.23	Rutin (μg/mL)	808.467
Time (h)	6.37	Quercetin (μg/mL)	193.296
Ethanol concentration (%)	75.04	Myricetin (μg/mL)	37.36

was no significant difference between the predicted and actual values. RSM indicated no difference between the predicted and actual values of quercetin. Myricetin content displayed a lower value than the predicted value and had a significant difference.

3.4. Conclusion

This study aimed to optimize the extraction conditions of the rutin, quercetin, and myricetin flavonoids from tartary buckwheat sprouts using RSM. A Box-Behnken design containing 15 experiments was employed to evaluate the effect of extraction conditions that included temperature (X_1, 50-70°C), extraction time (X_2, 5-9 h), and ethanol concentration (X_3, 60-90%). The optimal extraction conditions that maximized rutin, quercetin, and myricetin contents were obtained at X_1=51.03, X_2=6.62, and X_3=69.16%. Under the optimal conditions, the predicted rutin, quercetin, and myricetin contents were 808.467, 193.296, and 37.360 µg/mL, respectively. Ten experiments were performed to validate the model. The experimental values of rutin and quercetin contents were similar to the predicted values. However, the experimental value of myricetin content was less than the predicted value.

3.5. References

Aguirre L, Arias N, Teresa Macarulla M, Gracia A, Portillo M. 2011. Beneficial effects of quercetin on obesity and diabetes. The Open Nutraceuticals Journal, 4, 189–198.

Boots AW, Li H, Schins RP, Duffin R, Heemskerk JW, Bast A, Haenen GR. 2007. The quercetin paradox. Toxicology and Applied Pharmacology, 222, 89-96.

Carocho M, Ferreira IC. 2013. A review on antioxidants, prooxidants and related controversy: natural and synthetic compounds, screening and analysis methodologies and future perspectives. Food and Chemical Toxicology, 51, 15-25.

Chua LS. 2013. A review on plant-based rutin extraction methods and its pharmacological activities. Journal of Ethnopharmacology, 150, 805-817.

Davis JM, Murphy EA, Carmichael MD. 2009. Effects of the dietary flavonoid quercetin upon performance and health. Current Sports Medicine Reports, 8, 206-213.

Davis JM, Zhao Z, Stock HS, Mehl KA, Buggy J, Hand GA. 2003. Central nervous system effects of caffeine and adenosine on fatigue.

American Journal of Physiology-Regulatory, Integrative and Comparative Physiology. 208, 399-404.

Fabjan N, Rode J, Kosir IJ, Wang Z, Zhang Z, Kreft I. 2003. Tartary buckwheat (*Fagopyrum tataricum* Gaertn.) as a source of dietary rutin and quercitrin. Journal of Agricultural and Food Chemistry, 51, 6452-6455.

Harwood M, Danielewska-Nikiel B, Borzelleca JF, Flamm GW, Williams GM, Lines TC. 2007. A critical review of the data related to the safety of quercetin and lack of evidence of *in vivo* toxicity, including lack of genotoxic/carcinogenic properties. Food and Chemical Toxicology, 45, 2179-2205.

Heo H, Lee H, Kim Y, Jeong HS, Lee J. 2019. Optimization of ultrasound-assisted extraction of antioxidant compounds from onion peels using response surface methodology. Journal of The Korean Society of Food Science and Nutrition. 48, 441-446.

Jang M, Asnin L, Nile SH, Keum YS, Kim HY, Park SW. 2013. Ultrasound-assisted extraction of quercetin from onion solid wastes. International Journal of Food Science & Technology, 48, 246-252.

Kang NJ. 2015. Rutin Suppresses Neoplastic Cell Transformation by Inhibiting ERK and JNK Signaling Pathways. The Korean Journal of Food and Nutrition, 28, 579-585.

Kwon TB. 1994. Change in rutin and fatty acids buckwheat during germination. The Korean Journal of Food and Nutrition. 7, 124-127.

Kraujalis P, Venskutonis PR, Ibanez E, Herrero M. 2015. Optimization of rutin isolation from *Amaranthus paniculatus* leaves by high pressure extraction and fractionation techniques. The Journal of Supercritical Fluids, 104, 234-242.

Kreft I, Fabjan N, Yasumoto K. 2006. Rutin content in buckwheat (*Fagopyrum esculentum* Moench) food materials and products. Food Chemistry, 98, 508-512.

Liu CL, Chen YS, Yang JH, Chiang BH. 2008. Antioxidant activity of tartary (*Fagopyrum tataricum* (L.) Gaertn.) and common (*Fagopyrum esculentum* Moench) buckwheat sprouts. Journal of Agricultural and Food Chemistry, 56, 173-178.

Mukhtar H, Das M, Khan WA, Wang ZY, Bik DP, Bickers DR. 1988. Exceptional activity of tannic acid among naturally occurring plant phenols in protecting against 7, 12-dimethylbenz (a) anthracene-,

benzo (a) pyrene-, 3-methylcholanthrene-, and N-methyl-N-nitrosourea-induced skin tumorigenesis in mice. Cancer Research, 48, 2361-2365.

Ong KC, Khoo HE. 1997. Biological effects of myricetin. General Pharmacology: The Vascular System, 29, 121-126.

Przybylski R, Lee YC, Eskin NAM. 1998. Antioxidant and radical-scavenging activities of buckwheat seed components. Journal of the American Oil Chemists' Society, 75, 1595.

Utesch D, Feige K, Dasenbrock J, Broschard TH, Harwood M., Danielewska-Nikiel B, Lines TC. 2008. Evaluation of the potential *in vivo* genotoxicity of quercetin. Mutation Research / Genetic Toxicology and Environmental Mutagenesis, 654, 38-44.

Zhang ZL, Zhou ML, Tang Y, Li FL, Tang YX, Shao JR, Xue WT, Wu YM. 2012. Bioactive compounds in functional buckwheat food. Food Research International, 49, 389-395.

Chapter 4. Bioconversion of flavonoid extracted from tartary buckwheat sprouts

Abstract

Four strains were isolated from buckwheat farmland in Pyeongchang, Kangwon-do: *Oxalobacteraceae bacterium* NR186, *Massilia suwonensis* strain PgBE21, *Massilia* sp. strain NEAU-DD11, and *Bacillus licheniformis* strain IND706. Only strain 3P-1, which had 98.97% similarity to *Bacillus licheniformis* strain IND706, could use the flavonoid during fermentation. During the 7 days of fermentation, the quercetin content decreased, rutin content slightly increased, and an unknown compound increased. The molecular weight of the unknown compound was analyzed by HPLC/MS. Among four candidate substances, isoquercetin was the most suitable considering the biosynthesis pathway, substrate, and characteristics of strain 3P-1.

4.1. Introduction

Flavonoids are mainly found in plants as *O*-glycosides bound to sugars that include glucose, galactose, rhamnose, arabinose, and xylose. Microbial fermentation had been broadly used for the biotransformation of flavonoids (Nguyen et al., 2018). Especially, microbial β-glycosidase breaks the *O*-β-glycosidic bonds of flavonoids to product aglycon, daidzein, genistein, and glycitein (Di Gioia et al., 2014). The bacterial transformation is necessary for flavonoid absorption and functional properties (Jou et al., 2013). The deglycosylation of flavonoids is induced by bacteria that produce enzymes such as cellulase, pectinase, and β-glucosidase (Zheng et al., 2000; Hur et al., 2014).

Studies have sought to improve flavonoid bioavailability and solubility. An enzyme isolated and purified from bacteria could hydrolyze and produce a different form of flavonoids could enhance their solubility, bioavailability, and functionality. Kaempferol-3-glucoside and quercetin-3-glucoside can be by *Bifidobacterium pseudocatenulatum* and *Aspergillus awamori*, respectively, resulting in the production of aglycon (Lin et al., 2014; Di Gioia et al., 2014)

This study's main objective was to investigate the potential ability of

the isolated strain to produce new flavonoids using extracts of tartary buckwheat sprouts. The enhanced functionality was confirmed by evaluating some bioactivities.

4.2. Materials and methods

4.2.1. Materials

Soil for isolation and identification of bacteria was collected from various sites on a buckwheat farmland in Pyeongchang, Kangwon-do. The collected soil was stored in a refrigerator (4℃) until required.

4.2.2. Reagents and culture media

Quercetin and rutin that were used as bioconversion resources were purchased from Sigma-Aldrich. For the isolation of bacteria, YPDA (Difco Laboratories, Becton, Dickinson and Company, Sparks, MD, USA), Tryptic soy agar (TSA; Difco Laboratories), and Nutrient agar (NA; Difco Laboratories) were used. Nutrient broth and tryptic soy broth were from Difco Laboratories. R2A media (MB cell, Seoul, Republic of Korea), Muller-Hinton broth (Oxoid Ltd., Basingstoke, UK), and other media were used in various tests to identify and characterize isolated bacteria.

API ZYM and API CHB were purchased from bioMerieux (Marcy-l'Étoile, France) to evaluate biochemical characteristics.

4.2.3. Isolation of bacteria

Soil sample (2 g) was suspended in phosphate buffered saline. The bacterial suspension was diluted by 10^{-1} and 10^{-2}. Aliquots of the diluted suspensions were inoculated in selective media, YPD agar, TSA, and R2A. The inoculated media were incubated at 30℃ for 3 days. Colonies of the strains displayed different morphological characteristics. Four strains were screened according to morphology.

4.2.4. PCR amplification and sequencing

To identify the bacteria, the 16s RNA gene of isolates of each strain was analyzed (Ponnusamy et al., 2008). The gene extraction was performed using the Accuprep® Genomic DNA extraction kit (Bioneer, Daejeon, Republic of Korea) according to the manufacturer's instruction.

For the PCR amplification, universal primer, 14F (AGAGTTTGATCCTGGCTCAG), and reverse 1492R (GGTTACCTTG TTACGACTT) was used. The PCR mixture consisted of 2 μL of template

DNA, 1 μL of each primer (0.2 μmol concentrations) and prime tag premix (G-3000; GeNet bio, Daejeon, Republic of Korea). Six microliters of sterile deionized water was added to achieve a final volume of 20 μL. Strain 3P-1 could not be analyzed by sequencing with universal primer (27F, 1492R) due to a frameshift. The forward primer was redesigned to preventing the frameshift. The primer (TAAACGATGAGTGCTAAGT) was designated 3P-F.

PCR reaction performed using the AllInOneCycler™ (Bioneer). After an initial step at 94°C for 5 min, 35 cycles of amplification were carried out. Each amplification cycle consisted of 30 s at 94°C, 30 s at 50°C, and 30 s at 72°C. A final extension step was performed for 10 min at 72°C. Two microliters of the PCR product were electrophoresed in 1.5% agarose gel with EcoDye Nucleic acid Staining Solution (Biofact). The amplified PCR products on the agarose gel were purified using a kit (Bioneer) according to the manufacturer's instructions. The nucleotide sequencing of the 16S rRNA gene fragments was performed by Bioneer. The sequencing results were analyzed by BioEdit software (http: //www.mbio. ncsu.edu/BioEdit/) for alignment.

4.2.5. Biochemical characteristics of bacteria

Biochemical characteristics were measured using the API test (bioMérieux). API CHB kit and API ZYM were used to detect carbon sources, carbohydrate fermentation, and enzyme activities of isolated bacteria. API CHB was used to determine whether the bacteria could or could not ferment carbohydrates that included glycerol, erythritol D-arabinose, L- arabinose, ribose, D-xylose, L-xylose, adonitol, methyl-B-D-xylopyranoside, galactose, glucose, fructose, mannose, sorbose, rhamnose, dulcitol, inositol, mannitol, sorbitol, methyl-α-D-mannolyranoside, methyl-α-, D-glucoside, amygdalin, arbutin, esculin, salicin, cellobiose, maltose, lactose, melibiose, sucrose, trehalose, inulin melezitose, raffinose, starch, glycogen, xylitol, gentiobiose, D-turanose, D-xylose, D-tagatose, D-fucose, D-arabitol, L-arabitol, gluconate, 2-keto-gluconate, and 5-keto-gluconate). The API ZYM kit was used to detect specific enzyme usage. The enzymes evaluated by the kit are shown in Table 4.1.

All the API kits were used according to the manufacturer's instructions. Briefly, the bacteria were grown on different media, using API and NA for the CHB kit and liquid culture for the NE and ZYM kits.

Table 4.1. List of enzymes and their substrates in API ZYM

	Enzyme	Substrate
1	Control	
2	Alkaline phosphatase	2-naphthyl phosphate
3	Esterase	2-naphthyl butylate
4	Esterase lipase	2-naphthyl capy/late
5	Lipase	2-naphthyl myristate
6	Leucine acrylamidase	L-leucyl-2-naphthylamide
7	Valine acrylamidase	L-valvyl-2-naphthylamide
8	Crystine acrylamidase	L-crystyl-2-naphthylamide
9	Trypsin	N-benzoyl-DL-arginine-2-napthylamide
10	α-Chymotrypsin	N-glutaryl-phenylamine-2-napthylamide
11	Acid phosphatase	2-naphthyl phosphate
12	Naphtol-AS-BI-phosphohydrolase	Naphtol-AS-BI-phosphate
13	α-Galactosidase	6-Br-2-naphthyl- α-D-galactopyraooside
14	β-Glucuronidase	2-naphthyl- β -D-galactopyranoside
15	β-Glucosidase	Naphthol-AS-BI- β-D-glucuronide
16	α-Glucosidase	6-Br-2-naphthyl- β -D-glucopyranoside
17	β-Glucosidase	Naphthol-AS-BI-β-D-glucopyranoside
18	N-Acetyl- β-glucosaminidase	1-naphtyl-N-acetyl-β-D-glucosaminide
19	α-Mannosidase	1-Br-2-naphthyl-
20	α-Fucosidase	2-naphthyl- α-L-fucopyranosied

The bacteria were diluted for each reaction with 0.85% NaCl. The bacteria that were well diluted for the purpose were inoculated into reservoirs of the API strip. If needed, another reagent was mixed with diluted bacteria before inoculation into the API strip. After incubation for the proper temperature and time, API results were determined by reading the color change.

4.2.6. Bioconversion of flavonoids and extract of tartary buckwheat sprouts

The isolated strains were examined for their bioconversion of flavonoids. Each strain was cultured in Muller-Hinton broth containing 200 ppm rutin, quercetin, and ethanolic extract concentrate of tartary buckwheat sprouts. The culture temperature was 35°C. Samples were collected every day for 7 days. The samples were stored in a freezer at -80°C and used to analyze rutin and quercetin contents. In addition, the aqueous and ethanolic extracts were added to the media for the bioconversion at 2% (v/v). The flavonoid content was measured using HPLC, as mentioned in section 2.2.6.

4.2.7. Conditions of HPLC/MS analysis

Flavonoids that did not exist before the fermentation products were found by flavonoid analysis using HPLC. HPLC/mass spectrometry (MS) analysis was performed to predict their molecular weights. Samples were analyzed by liquid chromatography/quantitative time-of-flight (LC/Q-TOF)/MS. The conditions of HPLC and MS analysis for ultra-performance liquid chromatography (UPLC) are summarized in Table 4.2. UPLC analysis was performed using an Acquity I-Class device (Milford, Taunton, MA, USA). Q-TOF MS analysis was performed using a maxis HD device (Bruker, Karlsruhe, Germany). The column temperature was 40°C, and 0.1% formic acid in water (A) and 0.1% formic acid in acetonitrile (B) were used. The flow rate was 0.4 mL/min.

4.3. Results and discussions

4.3.1. Isolation of bacteria converting flavonoids from querceetin

Four strains displayed distinct morphological characteristics. Three were isolated using TSA and one using YPDA. The isolated bacteria were

Table 4.2. Conditions of HPLC/MS analysis for unidentified flavonoids converted by the fermentation

Time (min)	A (0.1% Formic acid water)	B (0.1% Formic acid in acetonitrile)
0	99	1
2	99	1
12	20	80
16	0	100
18	0	100
19	99	1
21	99	1

designated 1P-1Y, 1P-1N, 1P-1T, and 3P-1. The morphologies on the solid media are shown in Fig. 4.1. 1P-1Y, 1P-1N, and 1P-1T were solid media are shown in Fig. 4.1. 1P-1Y, 1P-1N, and 1P-1T were Gram-negative. 3P-1 was Gram-positive. All were aerobic. 1P-1N colonies were milky white, convex, and round with clear margins. 1N-1T colonies were round two but were yellow. 1P-1Y colonies were opaque, irregular, and flat with a clear margin. 3P-1 colonies were white, filamentous, and irregular, with a dry surface was dry. A little mucoid substance was evident.

Table 4.3 summarizes data for the identification of isolated bacteria using 16s rRNA gene sequence analysis. 1P-1N displayed 98.87% similarity with *O. bacterium* NR186, 1P-1Y displayed 98.65% similarity with *M. suwonenesis* strain PgBE21. 1P-1T displayed 98.77% similarity with Massilia sp. Strain NEAU-DD11. *O. bacterium* and *Massilia* sp. were Gram-negative. *Masilla* sp. is widespread in nature, especially in soil. Its function was not well known through not many pieces of research.

Massilia sp. produces pigment (Agematu et al.,2011; Venil et al., 2020). *Masillia* sp. also was involved in *Oxalobacteraceae*. They are all Gram-negative bacteria. These prior findings were also found presently.
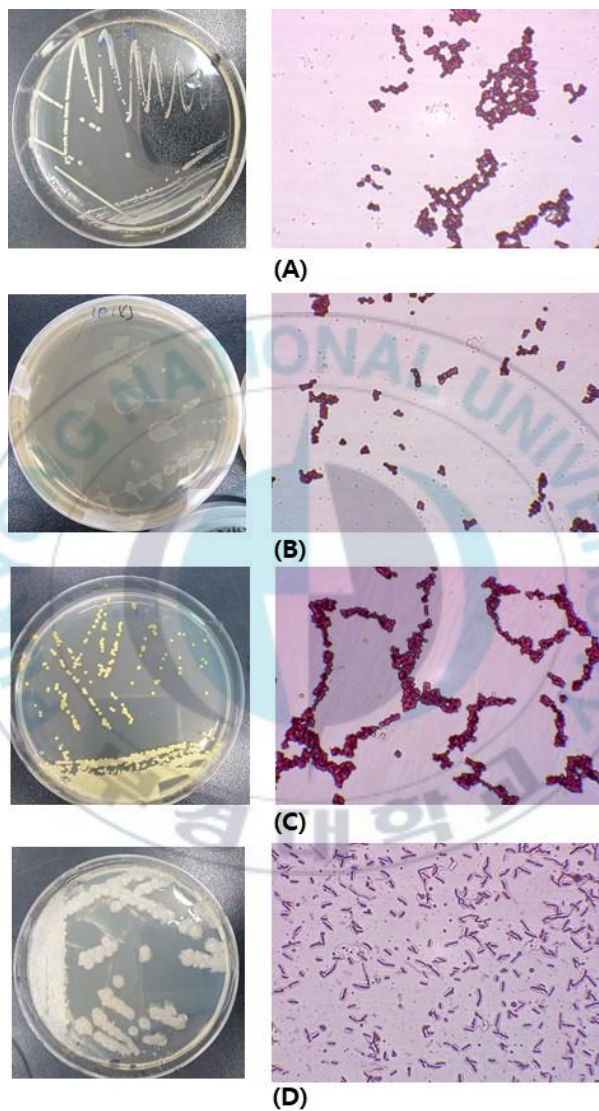
Fig. 4.1. Morphological characteristics of isolated bacteria

(A, 1P-1N; B, 1P-1Y; C, 1P-1T; D, 3P-1)

Table 4.3. Identification of the four strains based on 16s rRNA gene sequence analysis

	16S rRNA sequencing		
	Related strain in NCBI	Accession No.	Similarity (%)
1P-1N	*Oxalobacteraceae bacterium* NR186	MN784464.1	98.87
1P-1Y	*Massilia suwonensis* strain PgBE21	MN784464.1	98.65
1P-1T	*Massilia* sp. strain NEAU-DD11	MN784464.1	98.77
3P-1	*Bacillus licheniformis* strain IND706	MT642946.1	98.94

In contrast, 3P-1 displayed 98.94% similarity with *Bacillus licheniformis* strain IND 706. *B. licheniformis* is a Gram-positive bacterium that is common in soil. The four strains had similar morphologic characteristics as reported in previous studies.

Comparison with the sequence of NCBI strains revealed four phylogenetic trees in the neighbor-joining algorithm shown in Fig. 4.2 to 4.5. Each phylogenetic tree indicated the relationship between the particular novel strain and closely related species.

4.3.2. Biochemical analyses of the isolated bacteria

Table 4.4 presents the results of the API CHB tests. According to the sequencing results, different results were found in the biochemical tests using API. Among the three strains, 1P-1N fermented gluconate and 5-keto-gluconate. The strain also fermented different carbohydrates. CHB testing revealed that 1P-1Y and 1P-1T fermented the same carbon sources, which included glycerol, ribose, adonitol, rhamnose, N-acetyl-glucosamine, raffinose, D-fucose, and D-arabitol, unlike the 1P-1N strain. CHB API testing determined that the 1P-1N strain was a different bacterium from the 1P-1Y and 1P-1T strains. 1P-1Y and 1P-1T displayed
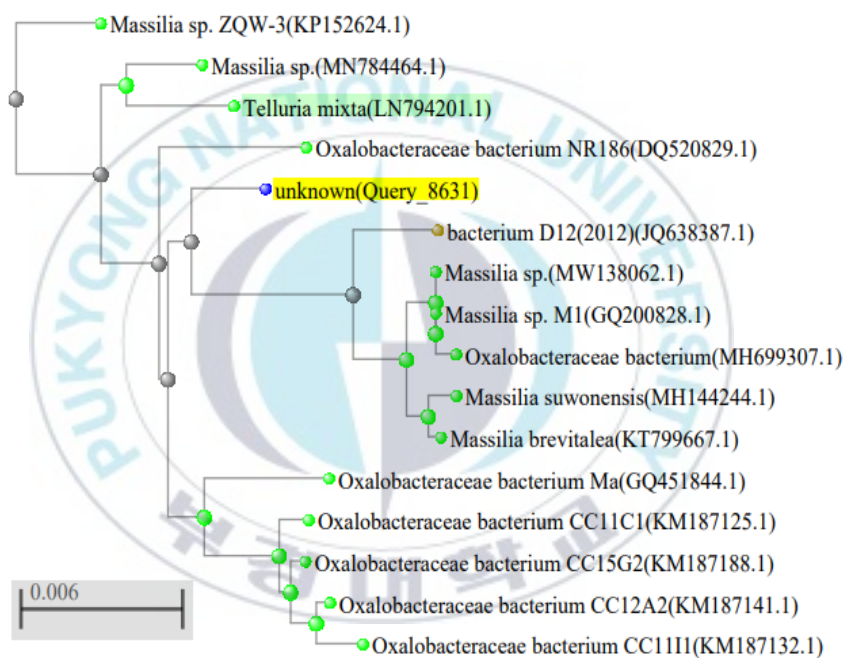
Fig. 4.2. Phylogenetic tree of strain 1P-1N based on analysis of 16S rRNA gene sequence.
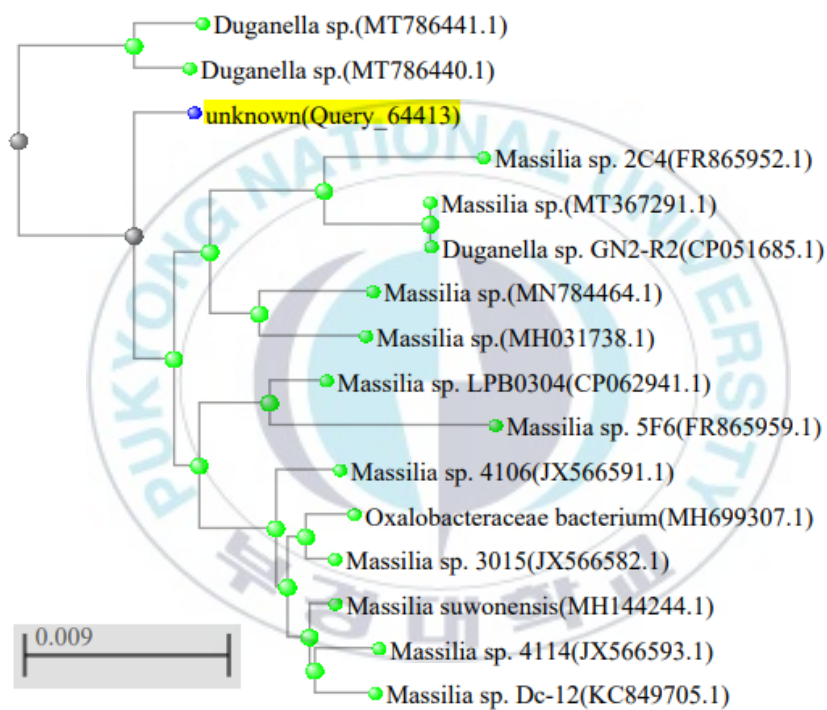
Fig. 4.3. Phylogenetic tree of strain 1P-1Y based on analysis of 16S rRNA gene sequence.
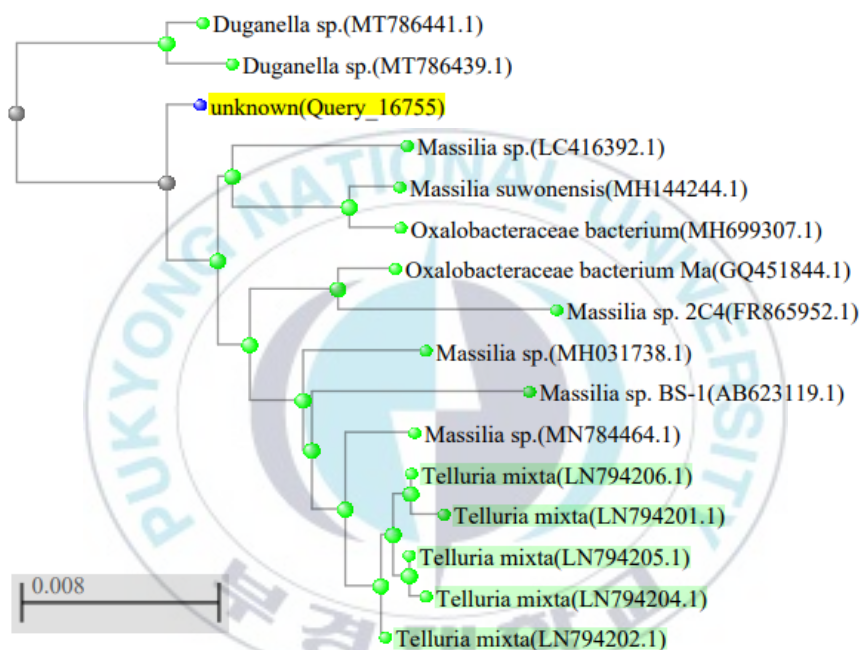
Fig. 4.4. Phylogenetic tree of strain 1P-1T based on analysis of 16S rRNA gene sequence.
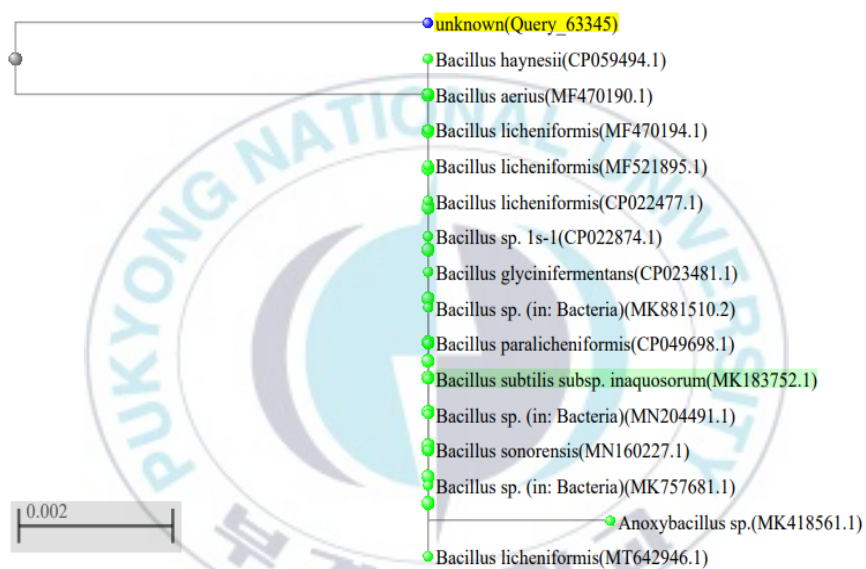
Fig. 4.5. Phylogenetic tree of strain 3P-1 based on analysis of 16S rRNA gene sequence.

**Table 4.4. Utilization of carbohydrate by the four isolated bacteria**

	Carbohydrate	1P-1N	1P-1Y	1P-1T	3P-1
1	Glycerol	+	+	+	+
2	Erythritol	-	-	-	-
3	D-Arabinose	-	-	-	-
4	L-Arabinose	+	+	+	+
5	Ribose	-	+	+	+
6	D-Xylose	+	+	+	+
7	L-Xylose	-	-	-	-
8	Adonitol	-	+	+	-
9	Methlyl-B-D-xylopyranside	-	-	-	-
10	Galactose	+	+	+	+
11	Glucose	+	+	+	+
12	Fructose	+	+	+	+
13	Mannose	+	+	+	+
14	Sorbose	+	+	+	+
15	Rhamnose	-	+	+	+
16	Dulcitol	-	-	-	-
17	Inositol	+	+	+	+
18	Mannitol	-	+	+	+
19	Sorbitol	+	+	+	+
20	Methyl-α-D-mannolyranside,	-	-	-	-

Continued

120

	Carbohydrate	1P-1N	1P-1Y	1P-1T	3P-1
21	Methyl-α-,D-glucoside	+	+	+	+
22	N-Acetyl-glucosamine	-	+	+	+
23	Amygdalin	-	-	-	+
24	Arbutin	+	+	+	+
25	Esculin	+	+	+	+
26	Slaicin	+	+	+	+
27	Cellobiose	-	+	+	+
28	Maltose	+	+	+	+
29	Lactose	+	+	+	+
30	Melibiose	+	+	+	+
31	Sucrose	+	+	+	+
32	Trehalose	+	+	+	+
33	Inulin	-	-	-	-
34	Melezitose	+	+	+	+
35	Raffinose	-	+	+	+
36	Starch	-	-	-	+
37	Glycogen	-	-	-	-
38	Xylitol	-	-	-	-
39	Gentiobiose	+	-	+	+
40	D-Turanose	-	-	-	-

Continued

	Carbohydrate	1P-1N	1P-1Y	1P-1T	3P-1
41	D-Xylose	-	-	-	-
42	D-Taratose	-	-	-	-
43	D-Fucose	-	+	+	+
44	D-Arabitol	-	+	+	+
45	L-Arabitol	-	+	+	-
46	Gluconate	+	-	-	+
47	2-Keto-gluconate	-	-	-	+
48	5-Keto-gluconate	+	-	-	+
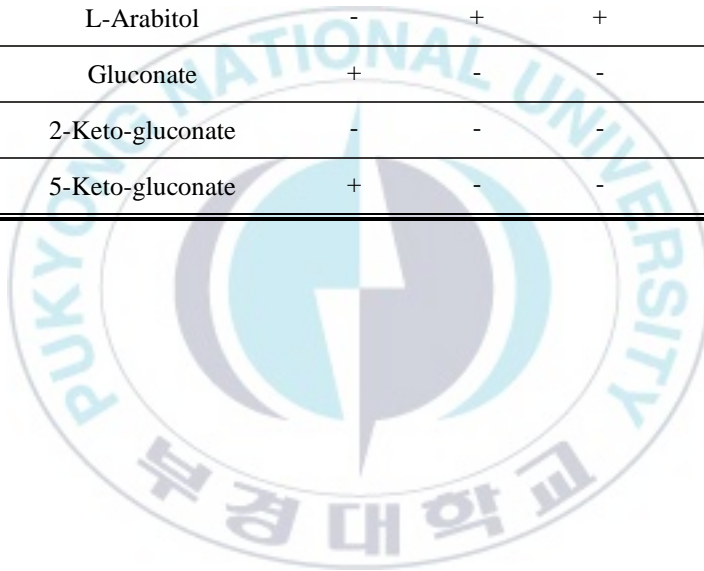
the identical pattern of carbohydrate fermentation. A prior study of *Massilia* sp. revealed that all seven strains could hydrolyze D-mannose and maltose, and D-glucose and L-arabinose would be fermented by six strains (Weon et al., 2008). Both the strains used in the present and previous studies were in the genus *Massilia* sp. The available carbon sources were different depending on the characteristics of each strain.

Strain 3P-1 strain could not ferment 14 of the 48 tested carbohydrates, which included erythritol, D-arabinose, L-xylose, adonitol, methyl-B-D-xylopyranside, dulcitol, methyl-α, D-mannolyranoside, iluin, glycogen, xylitol, D-turanose, D-xylose, D-taratose, and L-arabitol. The strain was thought to be a member of the genus *Massilia* sp. *Bacillus* sp. showed a significant difference in the pattern of fermentation. Table 4.5 presents the results of the API CHB tests. The 1P-1Y, 1P-1N, 1P-1T, and 3P-1 strains displayed different enzymatic activities. The 1P-1Y strain showed the highest acid phosphatase activity. The enzyme catalyzes the removal of phosphoryl groups from other molecules. The 1P-1N strain displayed alkaline phosphatase, leucine acrylamidase, naphthol-AS-BI phosphohydrolase, α-galactosidase, β-glucuronidase, and β-glucosidase activities. The 1P-1T strain displayed pronounced α-glucosidase activity.

In another study, all seven *Massilia* sp. were positive for alkaline phosphatase, esterase, esterase lipase, leucine arylamidase, valine arylamidase, acid phosphatase, and naphthol-AS-BIphosphohydrolase, but were negative for lipase, trypsin, α-chymotrypsin, β-glucuronidase, N-acetyl-b-glucosaminidase, α-mannosidase, and afucosidase (Weon et al., 2008). The 3P-1 strain was characterized by potent alkaline phosphatase and acid phosphatase activities. Weak lipase activity was evident.

4.3.3. Fermentation using isolated bacteria

Quercetin and rutin existed mainly in the tartary buckwheat sprouts. The bioconversion of these flavonoids by the four strains was assessed. Media contained 200 ppm rutin and quercetin, and a concentrate of ethanolic extracts. There was no significant change in fermentation by 1P-1N, 1P-1Y, and 1P-1Y. Bioconversion of quercetin by 3P-1 yielded a unidentified compound. The results of the HPLC analysis are shown in Fig. 4.6. Only the quercetin peak was evident prior to fermentation in Fig. 4.6. (A). After fermentation for 7 days, three prominent peaks were observed. One was the quercetin substrate at 8.77 min retention time. One peak was rutin at 6.8 min. Another peak with a difference of 0.26 min

Table 4.5. Level of enzymatic activities in the four isolated bacteria

	Enzyme	Score[1]			
		1P-1Y	1P-1N	1P-1T	3P-1
1	Control	-	-	-	-
2	Alkaline phosphaterase	3	5	2	5
3	Esterase	4	-	2	3
4	Esterase lipase	3-	-	2	1
5	Lipase	-	-	1	-
6	Leucine acrylamidase	-	3	5	2
7	Valine acrylamidase	-	-	1	-
8	Crystine acrylamidase	-	-	-	-
9	Trypsin	-	-	-	-
10	α-Chymotrypsin	-	-	-	2
11	Acid phosphatase	5	5	2	5
12	Naphtol-AS-BI-phosphohydrolase	3	4	3	3
13	α-Galactosidase	-	1	-	-

Continued

14	β-Glucoronidase	-	1	-	-
15	β-Glucosidase (Naphthol-AS-BI- β-D-glucuronide)	-	-	-	-
16	α-Glucosidase	-	2	5	4
17	β-Glucosidase (Naphthol-AS-BI-β-D-glucopyranoside)	-	3	-	4
18	N-Acetyl- β-glucosaminidase	-	-	-	-
19	α-Mannosidase	-	-	-	-
20	α-Fucosidase	-	-	-	-

[1] Score 5, very high enzyme activity; 4, high enzyme activity; 3, medium enzyme activity; 2, low enzyme activity; 1 very low enzyme activity
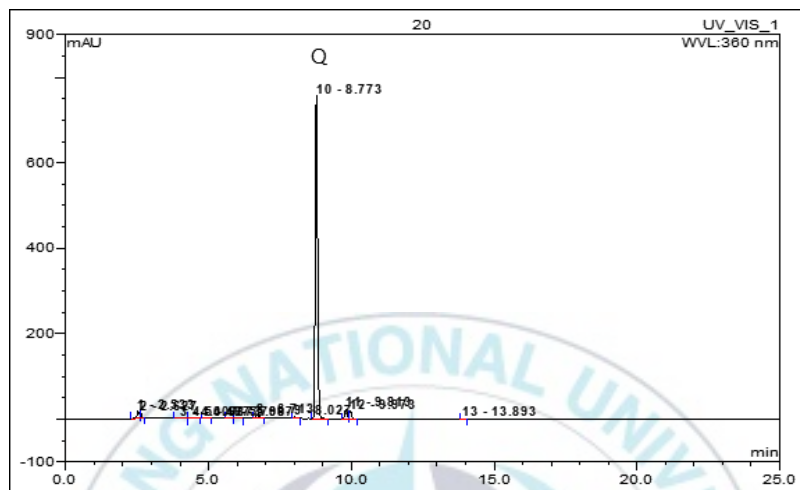
(A)
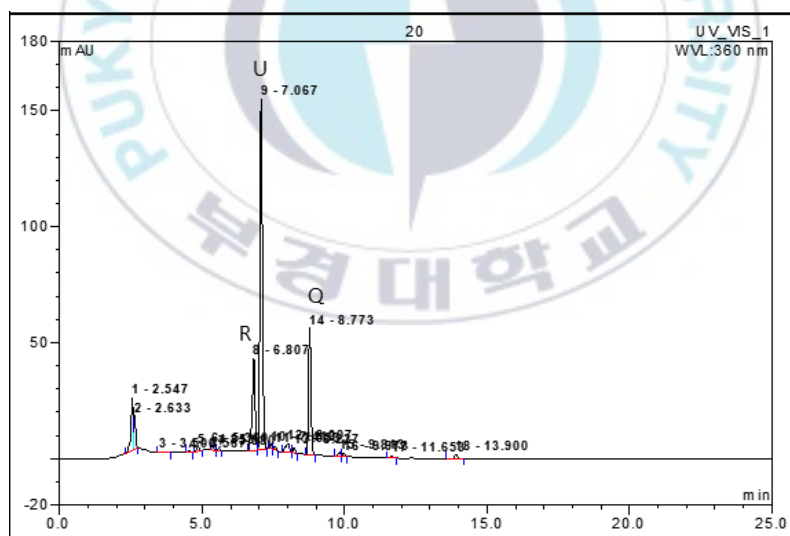
(B)

Fig. 4.6. HPLC analyses of quercetin before and after fermentation

(R, rutin; Q, quercetin, U, unknown)

from the rutin was the unidentified compound. The peak was clearly separated from the rutin peak, and it was confirmed that the amount of quercetin was evidently decreased. The absorbance of quercetin peak was approximately 800 on the first day of fermentation, but had decreased to 60 on day 7.

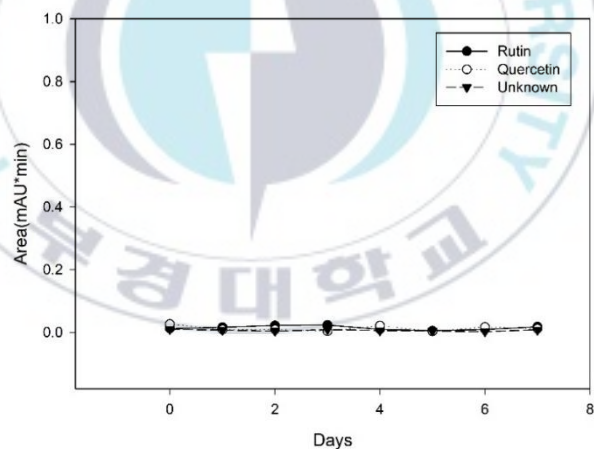### 4.3.4. Change of flavonoid contents during fermentation

The change of flavonoid content during fermentation is shown in Fig. 4.7 to 4.10. The unknown compound was not quantified with a standard substance. Thus, the flavonoid content was expressed as a peak area (mAU*min).

The results in Fig. 4.7 were controlled to evaluate whether strain 3P-1 could produce flavonoids. The flavonoid content did not change for 7 days. Thus, 3P-1 could not synthesize flavonoids in the absence of substrate.

Fig. 4.8 depicts the change in flavonoid content in the absence and presence (200 ppm) of quercetin by 3P-1. The quercetin content was the highest on the first day. Quercetin was insoluble in water and was added to the media to make an unsaturated state. Suspended quercetin was
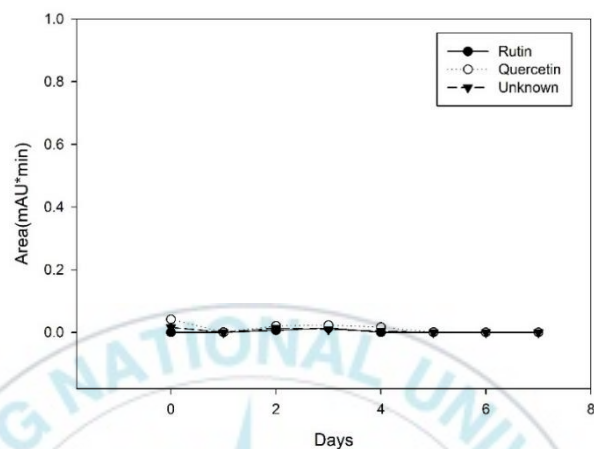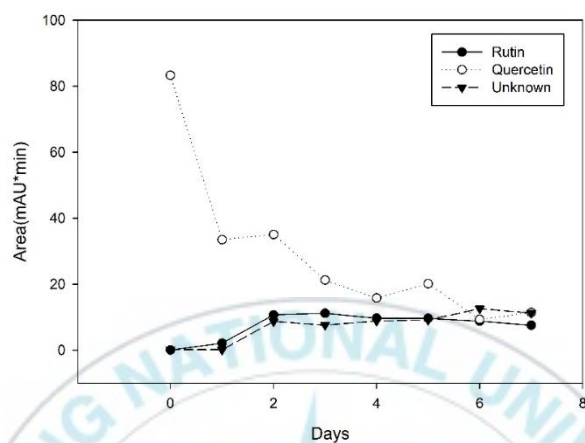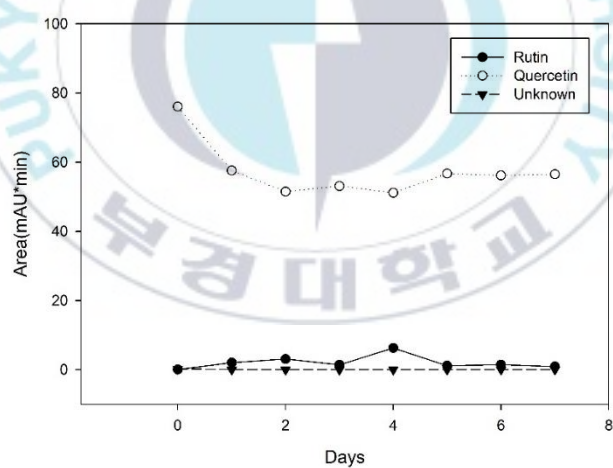
(A)

(B)

Fig. 4.7. Change of flavonoid contents on Muller-Hinton medium during fermentation with (A) and without (B) strain 3P-1
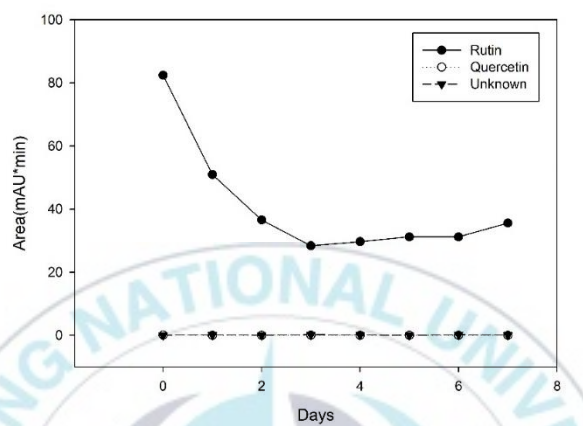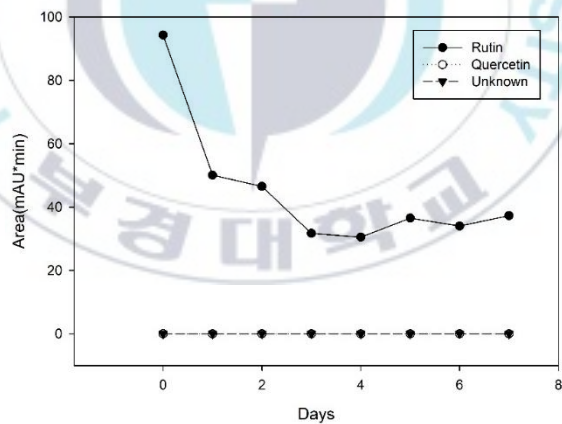
129

(A)

(B)

Fig. 4.8. Change of flavonoid contents on Muller-Hinton medium containing 200 ppm quercetin during fermentation with (A) and without (B) strain 3P-1

dissolved during the pre-treatment for HPLC analysis. After the first day of the process, quercetin content was decreased significantly. The contents of rutin and the unknown compound were increased in the samples containing 3P-1 and quercetin. The content of quercetin, rutin, and the unknown compound content was 83.28, 0, and 0 mAU*min, respectively, on the first day, and 11.45, 7.60, and 11.28 mAU*min, respectively, on day 7. The rutin content increased until day 4 and then decreased. In the medium lacking the strain 3P-1, the quercetin content was decreased, but the contents of rutin and the unknown compound did not change. For strain 3P-1, there was no change in the flavonoid contents (Fig. 4.8). Rutin was also slightly soluble in water, and displayed the same tendency as quercetin to be the highest on day 1 and dissolve during pre-treatment during HPLC analysis. Although the rutin content decreased, the content of the other compounds was not increased or was not evident. Fermentation with the concentrate of tartary buckwheat sprout ethanol and aqueous extracts did not affect flavonoid contents, as shown in Fig. 4.9 and 4.10. With a sufficient amount of quercetin, strain 3P-1 could produce the unidentified compound. Prior studies reported that *Bacillus* sp. ferment flavonoids and phenolic compounds (Huyuh et al., 2014b). *B. subtilis* can
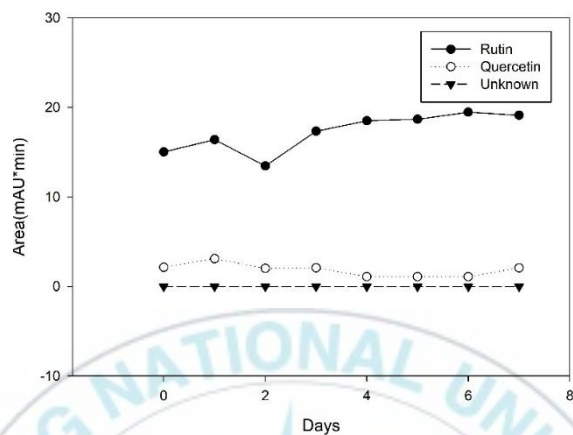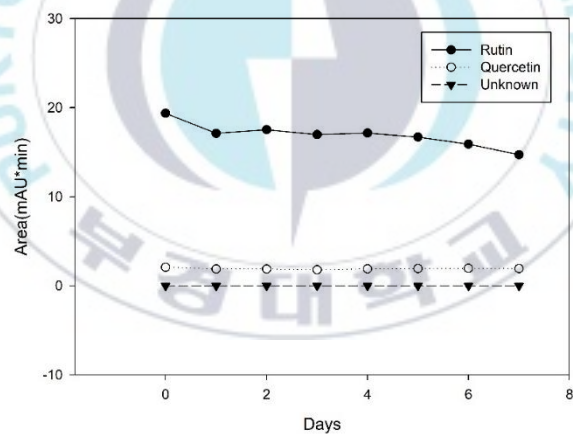
(A)

(B)

Fig. 4.9. Change of flavonoid contents on Muller-Hinton medium containing 200 ppm rutin during fermentation with (A) and without (B) strain 3P-1

(A)

(B)

Fig. 4.10. Change of flavonoid contents on Muller-Hinton medium containing 200 ppm ethanolic extract concentrate from tartary buckwheat sprouts during fermentation with (A) and without (B) strain 3P-1

133

produce daidzein and genistein in Cheonggukjang (soybean paste). During the fermentation of Cheonggukjang by *B. pumilus* HY1, the isoflavone aglycones, flavanols, and gallic acid were increased (Cho et al., 2009).

Also, *B. subtilis* fermentation of soybean yields chlorogenic acid and naringenin (Chung et al., 2011). *B. cereus* reportedly can convert quercetin to isoquercetin during the fermentation process with a yield of 20% (Rao et al., 1981). Other bacteria can also ferment quercetin, except for some *Bacillus* sp., to another form of flavonoid and phenolic compounds (Huyuh et al., 201b). Bioconversion of flavonoids is possible by microbial fermentation, including glycosylation and methylation. Enzymes produced by strain 3P-1 catalyzed the change of quercetin to another substance.

4.3.5. HPLC/MS analysis fermented flavonoid using isolated bacteria

The fermentation products were analyzed by HPLC, as mentioned in section 4.3.3. HPLC/MS analysis was performed for the unidentified compound to determine its molecular weight. Rutin and quercetin peaks analyzed by HPLC/MS were confirmed, as depicted in Fig. 4.11 and Fig.
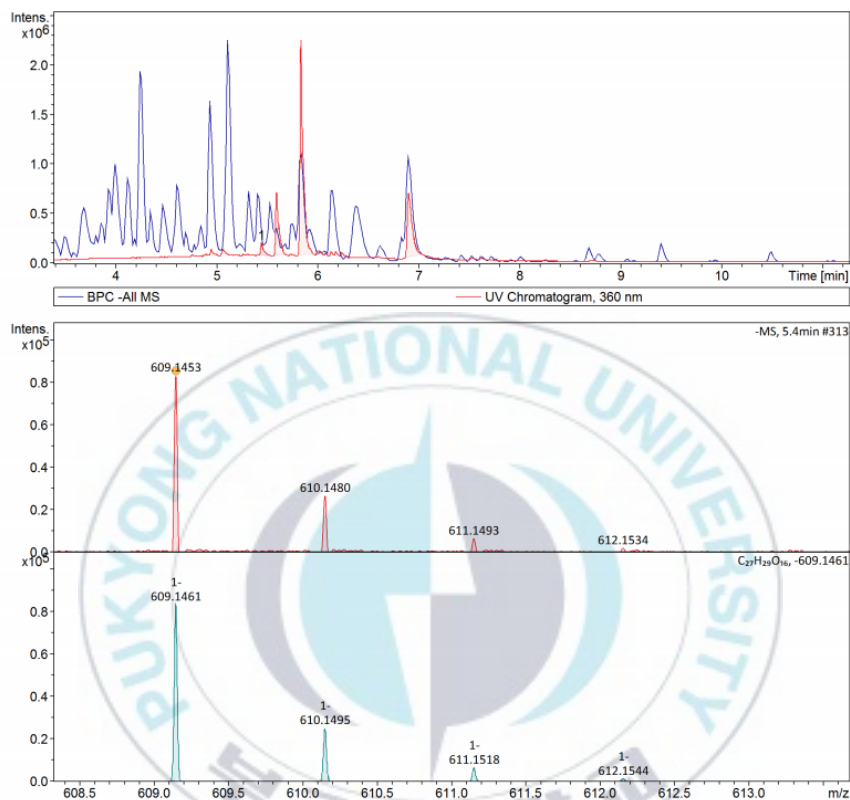
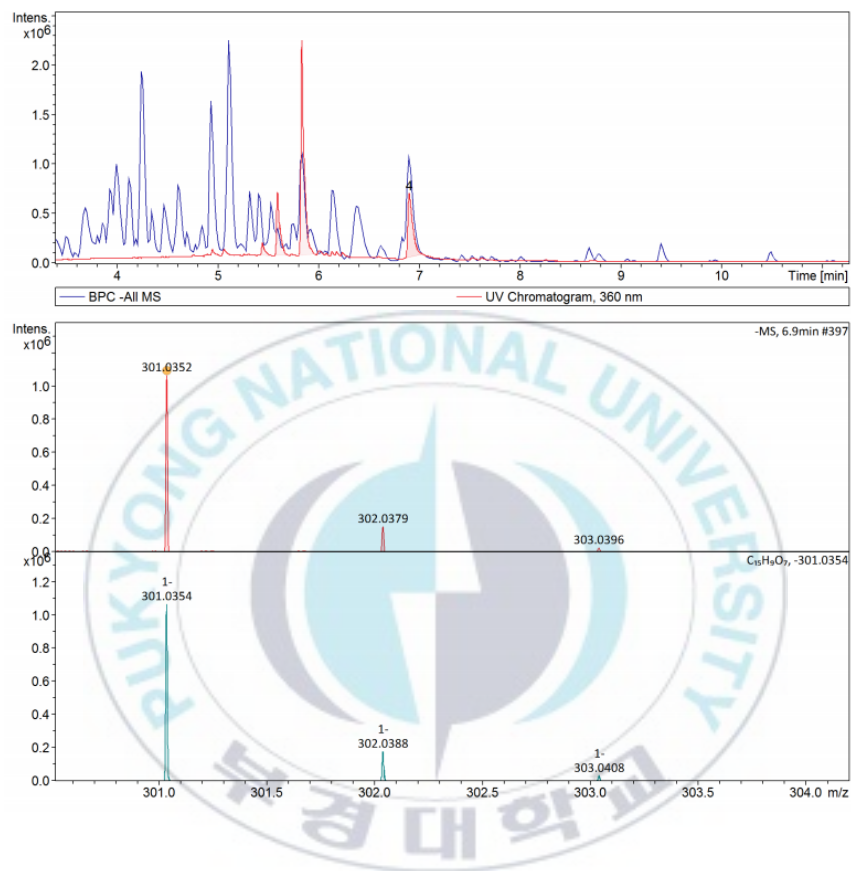**Fig. 4.11. Rutin peak of analysis by HPLC/MS.**

Fig. 4.12. Quercetin peak of analysis by HPLC/MS.

4.12. The novel peak evident in the HPLC analysis was separated into two

peaks (Fig. 4.13 and Fig. 4.14) at 5.6 and 5.8 min, in addition to rutin at

5.4 and quercetin at 6.9 min. According to the compound spectrum smart

formula report, the peak at 5.6 min was detected at 437.2754, 455.2130,

463.0872, and 586.2866 g/mol molecular weight. The peak at 5.8 min had

molecular weights of 463.0872 and 563.1039 g/mol . According to the

molecular weight, the chemical ion formula was determined in Table 4.6.

Thecompound was identified by a PubChem (https://pubchem.ncbi.

nlm.nih.gov/) search based on ion formula. The 463.0872 g/mol was

identified as four substances: myricetin 3-O-α-L-rhamnoside, quercetin-

3-O-galactoside (hyperaside), quercetin-3-glucoside (isoquercetin), and

delfinidin-3-O-glucoside. Myricetin 3-O-α-L-rhamnoside is synthesized

from myricetin and UDP-β-L-rhamnose (UDP, Uridine

diphosphate). Quercetin3-O-galactoside is synthesized from quercetin

and UDP- α-D-galactose by activation of quercetin-O-glucosyltransferase.

Delphinidin-3-O-glucoside is synthesized using UDP-α-D-glucose and

delphinidin by activating anthocyanidin 3-O-glucosyltransferase in the

anthocyanin biosynthesis pathway. Quercetin-3-glucoside is synthesized

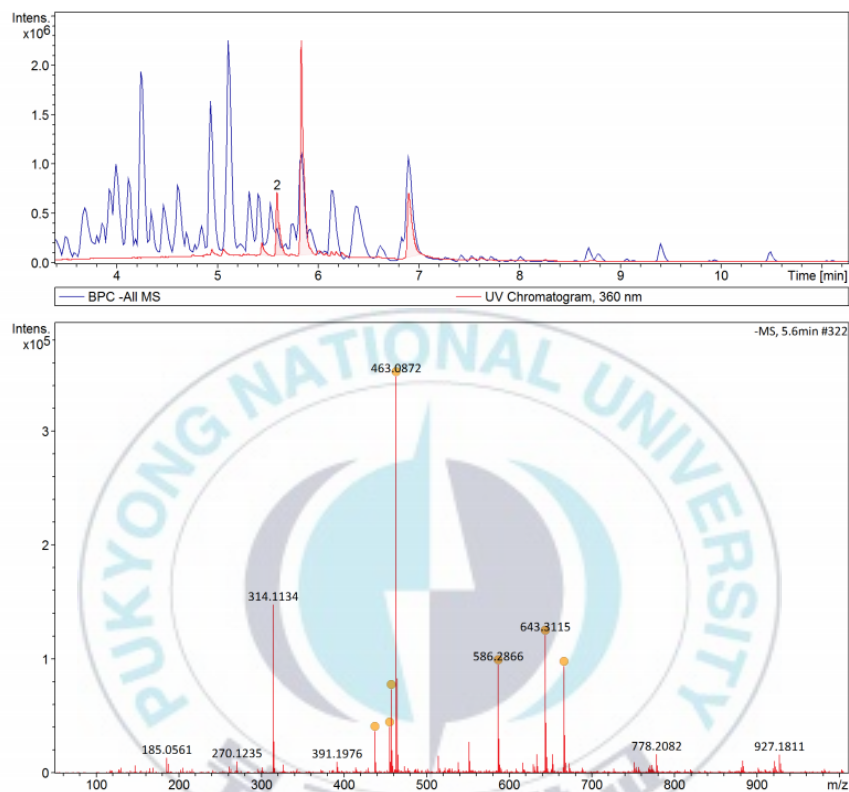from the quercetin glucoside biosynthesis of quercetin and UDP-α-D-

137

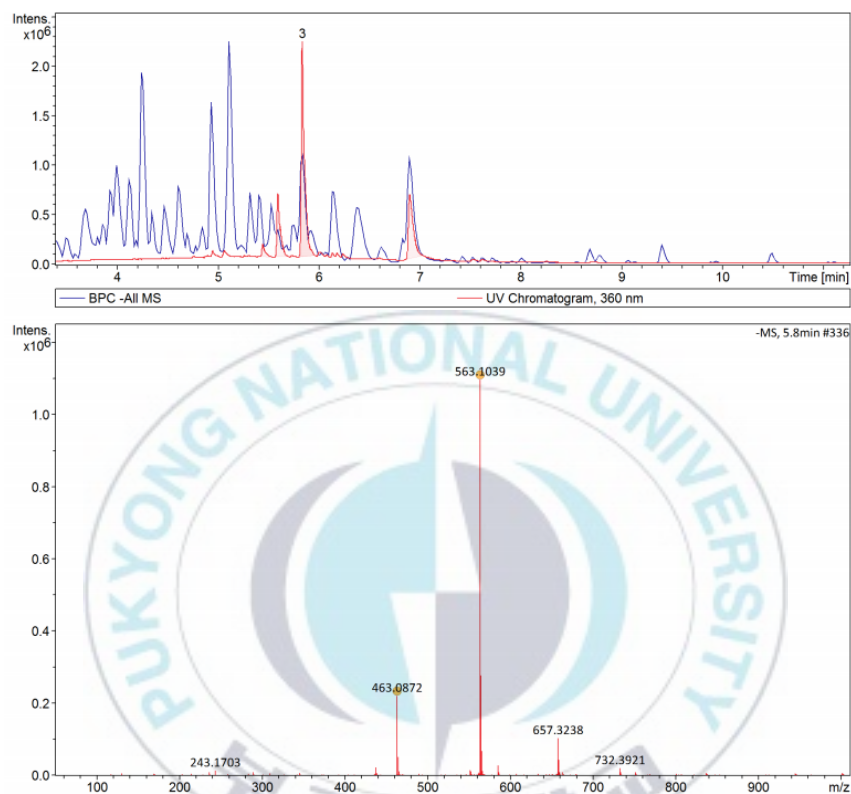**Fig. 4.13. HPLC/MS analysis of unidentified compound (I) after fermentation by isolated bacteria.**

Fig. 4.14. HPLC/MS analysis of unidentified compound (II) after fermentation by isolated bacteria.

Table 4.6. Putative chemical compositions of unidentified compound I and II based on HPLC/MS

Retention time	Putative molecular weight (m/z)	Putative chemical compositions	Putative molecular weight based on ion formula
5.6	437.275	$C_{21}H_{41}O_9$	437.2756
	455.2130	$C_{17}H_{23}N_{14}O_2$	455.2134
		$C_{16}H_{27}N_{10}O_6$	455.2121
		$C_{19}H_{35}O_{12}$	455.2134
	457.2440	$C_{23}H_{37}O_9$	457.2443
	463.0872	$C_{21}H_{19}O_{12}$	463.0882
		$C_{18}H_{11}N_{10}O_6$	463.0869
		$C_{19}H_7N_{14}O_2$	463.0882
	586.2866	$C_{28}H_{44}NO_{12}$	586.2869
		$C_{25}H_{36}N_{11}O_6$	586.2856
		$C_{26}H_{32}N_{15}O_2$	586.2869
	643.3115	$C_{32}H_{39}N_{10}O_5$	643.3110
		$C_{33}H_{35}N_{14}O$	643.3124
	666.3451	$C_{27}H_{40}N_{17}O_4$	666.3455
		$C_{26}H_{44}N_{13}O_8$	666.3441
5.8	463.0872	$C_{21}H_{19}O_{12}$	463.0882
		$C_{18}H_{11}N_{10}O_6$	463.0869
		$C_{19}H_7N_{14}O_2$	463.0882
	563.1039	$C_{22}H_{15}N_{10}O_9$	563.1029
		$C_{23}H_{11}N_{14}O_5$	563.1042
		$C_{25}H_{23}O_{15}$	563.1042

glucose by activation of quercetin-3-O-glucosyltransferase and rutin degradation.

Considering all the conditions, including the substrate and changes in flavonoid contents, quercetin-3-glucoside (isoquercetin) was the most suitable compound for the fermentation conditions.

Quercetin was converted to isoquercetin as catalyzed by isoquercetin synthase. Isoquercetin is converted to rutin as catalyzed by rutin synthase (Lucci and Mazzafera. 2009). *B. cereus* converts quercetin to isoquercetin through microbial metabolism during the fermentation process, with a yield of 20%. However, *B. cereus* does not convert rutin to isoquercetin (Rao et al., 1981). The same findings were obtained in the present. Thus, isoquercetin was synthesized by glucosidation of quercetin.

4.4. Conclusion

Four strains were isolated from a buckwheat farmland in Pyeongchang, Kangwon-do, based on their morphological characteristics. These strains were identified as 16s rRNA gene sequence analysis as *O. bacterium* NR186*, M. suwonensis* strain PgBE21, *Massilia* sp. strain

NEAU-DD11, and *B. licheniformis* strain IND706, with a similarity of 98.65 to 98.94%. Among them, only strain 3P-1, which had 98.97% similarity with *B. licheniformis* strain IND706, utilized flavonoids during fermentation. During the 7 days of fermentation, the quercetin content decreased, the rutin content slightly increased, and the content of the unidentified compound increased. The molecular weight of the unidentified compound was determined by HPLC/MS. Four candidate substances were appeared compared with PubChem data. Isoquercetin was the most suitable considering the biosynthesis pathway, substrate, and characteristics of the strain.

4.5. References

Agematu H, Suzuki K, Tsuya H. 2011. *Massilia* sp. BS-1, a novel violacein-producing bacterium isolated from soil. Bioscience, Biotechnology, and Biochemistry, 75, 2008-2010.

Chung IM, Seo SH, Ahn JK, Kim SH. 2011. Effect of processing, fermentation, and aging treatment to content and profile of phenolic compounds in soybean seed, soy curd and soy paste. Food Chemistry, 127, 960-967.

Cho KM, Hong SY, Math RK, Lee JH, Kambiranda DM, Kim JM, Yun HD. 2009. Biotransformation of phenolics (isoflavones, flavanols and phenolic acids) during the fermentation of cheonggukjang *by Bacillus pumilus* HY1. Food Chemistry, 114, 413-419.

Di Gioia D, Strahsburger E, de Lacey AML, Bregola V, Marotti I, Aloisio I, Dinelli G. 2014. Flavonoid bioconversion in *Bifidobacterium pseudocatenulatum* B7003: A potential probiotic strain for functional food development. Journal of Functional Foods, *7*, 671-679.

Hur SJ, Lee SY, Kim YC, Choi I, Kim GB. 2014. Effect of fermentation on the antioxidant activity in plant-based foods. Food Chemistry, 160, 346-356.

Huynh NT, Smagghe G, Gonzales GB, Van Camp J, Raes K. 2018. Bioconversion of Kaempferol and Quercetin Glucosides from Plant Sources Using *Rhizopus* spp. Fermentation, 4, 102.

Huynh NT, Van Camp J, Smagghe G, Raes K. 2014. Improved release and metabolism of flavonoids by steered fermentation processes: a review. International Journal of Molecular Sciences, 15, 19369-19388.

Jou HJ, Tsai PJ, Tu JH, Wu WH. 2013. Stinky tofu as a rich source of

bioavailable S-equol in Asian diets. Journal of Functional Foods, 5, 651-659.

Lin S, Zhu Q, Wen L, Yang B, Jiang G, Gao H, Jiang Y. 2014. Production of quercetin, kaempferol and their glycosidic derivatives from the aqueous-organic extracted residue of litchi pericarp with *Aspergillus awamori*. Food Chemistry, 145, 220-227.

Lucci N, Mazzafera P. 2009. Rutin synthase in fava d'anta: purification and influence of stressors. Canadian Journal of Plant Science, 89, 895-902.

Ponnusamy L, Xu N, Nojima S, Wesson DM., Schal C, Apperson CS. 2008. Identification of bacteria and bacteria-associated chemical cues that mediate oviposition site preferences by Aedes aegypti. Proceedings of the National Academy of Sciences, 105, 9262-9267.

Rao KV, Weisner NT. 1981. Microbial transformation of quercetin by *Bacillus cereus*. Applied and Environmental Microbiology, 42, 450-452.

Venil CK, Dufosse L, Renuka Devi P. 2020. Bacterial pigments: sustainable compounds with market potential for pharma and food

industry. Frontiers in Sustainable Food Systems, 4, 100.

Weon HY, Kim BY, Son JA, Jang HB, Hong SK, Go SJ, Kwon SW. 2008. *Massilia aerilata* sp. nov., isolated from an air sample. International Journal of Systematic and Evolutionary microbiology, 58, 1422-1425.

Zheng Z, Shetty K. 2000. Solid-state bioconversion of phenolics from cranberry pomace and role of *Lentinus edodes* β-glucosidase. Journal of Agricultural and Food Chemistry, 48, 895-900.
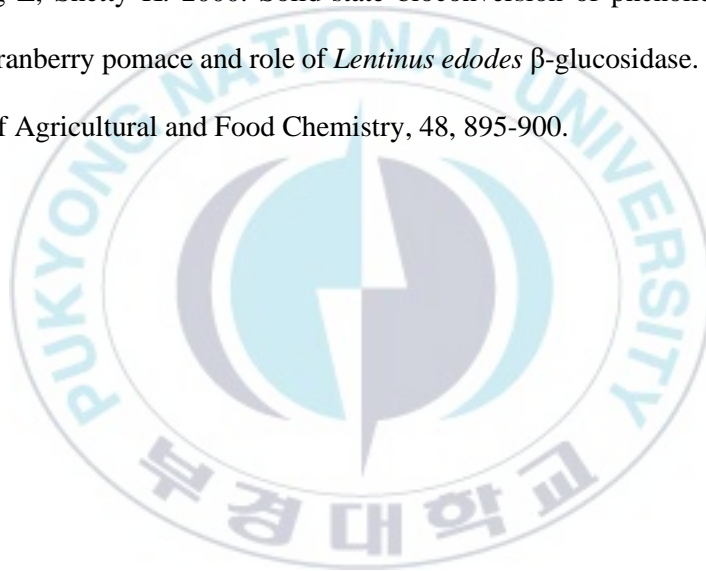
Summary

In this study, the flavonoid content of tartary buckwheat was improved through germination, optimized extraction, and biotransformation.

Initially, the germination conditions were controlled and changed to increase flavonoids tartary buckwheat sprouts. Excluding the primary conditions of moisture, oxygen, and temperature, the experiment was conducted by varying the intensity of light that can affect the formation of trace elements. The intensity of light varied from 0 to 18,000 lux. The contents of rutin, quercetin, myricetin, and kaempferol tended to increase until the light intensity reached 6,000 lux. In a similar trend, the contents of total flavonoids polyphenols content also increased, as did antioxidant activity. However, the antidiabetic and anticholesterol activities, which measure physiological activity through enzyme inhibitory activity, decreased. Different substances other than flavonoids displayed anti-diabetic and anti-cholesterol action, unlike antioxidant activity. Using the above conditions, the production conditions for tartary buckwheat sprouts were set using the smart farm system to enable mass production. In the

smart farm system, for products that can be used as food, conditions that could inhibit the growth of harmful microorganisms like mold, various conditions to control moisture, and chlorine disinfection conditions were different. Ultimately, a defined buckwheat density and slope that allowed sufficient moisture to be drained were established as the optimal conditions. Additional chlorine disinfection did not significantly affect the yield. Measurements of flavonoid contents revealed no differences according to each condition.

RSM was used to establish optimal conditions for extracting flavonoids from cultivated tartary buckwheat sprouts. Temperature, ethanol concentration, and extraction time were set as independent variables, and values were obtained through 15 experimental conditions using the Box-Benhen Design. The model set through each experiment presented a value that was sufficient to explain each content. The conditions enabling maximal yields of rutin, quercetin, and myricetin were extraction for 6.62 h using 69.13% ethanol at 51.03°C. The predicted values were 808.467 μg/mL for rutin, 193.296 μg/mL for quercetin, and 37.36 μg/mL for myricetin. As verification, 10 repeated experiments

revealed a slightly lower value that was sufficiently similar to the predicted value.

Four strains were isolated from a buckwheat field in Pyeongchang to increase the content of flavonoids through bioconversion using the extracted flavonoids or to obtain flavonoids having different functionalities. Among the four strains, 3P-1 fermented flavonoids. The strain was likely a *Bacillus* sp. When 3P-1 was used for fermentation in a medium containing 200 ppm quercetin, the content of quercetin gradually decreased and the amount of rutin increased for a certain period and then decreased. The molecular weight was determined by HPLC/MS. Analyses using various conditions revealed quercetin-3-O-glucoside as the most suitable compound.